

REVIEW ARTICLE

# Controlling the kinetics of interferon transgene expression for improved gene therapy

Kanitta Watcharanurak, Makiya Nishikawa, Yuki Takahashi, and Yoshinobu Takakura

Department of Biopharmaceutics and Drug Metabolism, Graduate School of Pharmaceutical Sciences, Kyoto University, Kyoto, Japan

---

## Abstract

Interferon (IFN) gene based therapy has been studied for the treatment of many diseases such as viral infections, cancer and allergic diseases. Non-viral vectors, like plasmid DNA, are promising ways for delivering IFN genes, because of their low immunogenicity and toxicity compared with viral vectors. Potent therapeutic effects of IFN gene transfer will depend on the level and duration of transgene expression after *in vivo* administration. Therefore, controlling the kinetics of transgene expression of IFNs is a rational approach for improved gene therapy. The design and optimization of plasmid vectors, as well as their route/method of administration, is the key to obtaining high and persistent transgene expression. In this review, we aim to present experimental evidence about the relationships among the properties of plasmid vectors expressing IFNs, the kinetics of transgene expression, and therapeutic effects as well as safety issues.

**Keywords:** Non-viral vector, plasmid DNA, CpG motifs, plasmid backbone, promoter, enhancer

---

## Introduction

Interferon (IFN) belongs to a family of cytokines, classified into three types based on the receptors with which they interact to initiate signal transduction. Type I IFN consists of many IFN subtypes including IFN- $\alpha$  and IFN- $\beta$ . Type I IFNs signal through an IFN- $\alpha$  receptor complex. IFN- $\gamma$  is the only IFN designated as a Type II IFN. IFN- $\gamma$  binds to an IFN- $\gamma$  receptor complex. The last and newest subgroup of IFNs, type III IFN, is IFN- $\lambda$ . IFN- $\lambda$  signals through a receptor complex consisting of IFN- $\lambda$  receptor 1 and Interleukin-10 receptor 2. All types of IFNs have been shown to exert immunomodulatory, antiviral and antiproliferative effects. IFNs have been extensively studied as a treatment for many diseases, such as viral infections, allergic diseases and cancer. However, the success of IFN-based therapy in clinical practice is limited probably because of the short *in vivo* half-life of IFN. Therefore, IFN gene transfer has been considered to be a promising alternative to overcome this hurdle as, theoretically, it should be able to supply IFN for a long period of time

(Platanias, 2005; Sadler & Williams, 2008; Bracarda et al., 2010; Kalanjeri & Serman, 2012).

Gene therapy is defined as the transfer of a gene of interest, such as a cytokine or an antigen, into the body to treat diseases. For over two decades since the first clinical trial of gene therapy in the late 1980s (Edelstein et al., 2007), gene therapy has shown great promise in treating a variety of diseases, such as cancer, cardiovascular diseases and inherited diseases. Gene transfer can be performed using vectors, which are generally categorized as viral and non-viral. Despite their high transfection efficacy, viral vectors are generally associated with serious toxicities, high immunogenicity and a limitation in the size of the transgene incorporated into the vector. Therefore, non-viral vectors, or non-viral gene delivery systems are very attractive alternatives because of their low toxicity, low immunogenicity, and ease of preparation without any limitation of DNA loading capacity. However, the main obstacle of non-viral vectors is the low and transient transgene expression, which prevents non-viral vectors

---

Address for Correspondence: Yoshinobu Takakura, PhD, Department of Biopharmaceutics and Drug Metabolism, Graduate School of Pharmaceutical Sciences, Kyoto University, 46-29 Yoshidashimoadachi-cho, Sakyo-ku, Kyoto 606-8501, Japan.  
E-mail: takakura@pharm.kyoto-u.ac.jp

(Received 25 June 2012; revised 21 July 2012; accepted 24 July 2012)

from exerting efficient therapeutic effects. To achieve efficient gene therapy, several advanced technologies have been developed to deliver plasmid DNA, the most frequently used non-viral vector, into target cells. This review provides an overview on current non-viral gene delivery methods, and summarizes the general ideas behind plasmid DNA modification for controlling the kinetics of transgene expression and some approaches that have been applied for IFN gene therapy in preclinical models.

### Non-viral gene delivery methods

Non-viral gene delivery methods have been summarized in many review articles (Nishikawa & Huang, 2001; Nishikawa & Hashida, 2002; Mehier-Humbert & Guy, 2005; Kamimura et al., 2011). Here, we briefly show some major methods that have been used for *in vivo* gene transfer using plasmid DNA.

Non-viral methods can be divided into two main categories, physical and chemical approaches. The physical approaches cover a local or systemic injection of naked plasmid DNA by a simple needle insertion and an injection together with the application of physical or electrical forces. The latter methods generate transient pores in the plasma membrane and enhance cell membrane permeability, thus the delivery of plasmid DNA into the cytoplasm is achieved. Besides the simple injection methods, such as intramuscular injection, intratumoral injection, and so on, other well-established physical methods include hydrodynamic injection method, gene gun and electroporation. The advantages of the physical methods are the simplicity and safety.

Chemical approaches are based on the use of synthetic or natural substances that form complex with plasmid DNA through, in most cases, electrostatic interaction. Because plasmid DNA is a negatively charged polyanion, positively charged compounds, such as cationic lipids and cationic polymers, are used to obtain lipoplex or polyplex, respectively. Some methods, which combine physical and chemical methods, such as ultrasound- or magnetic field-responsive compounds, have also been invented.

Among non-viral gene delivery methods, the simple injection of naked plasmid DNA is the most popular method in clinical situations. The latest gene therapy clinical trial data indicate that the number of clinical trials using naked plasmid DNA has increased from 14% in 2004 to 18.5% in 2012 (Edelstein et al., 2004; Edelstein et al., 2007; Edelstein, 2012).

### Optimization of plasmid DNA components

Two main components of plasmid DNA determine the extent of transgene expression as well as DNA production in bacteria. One is the gene control region, i.e., promoter and enhancer, which is required for regulating the transgene expression in eukaryotic cells. Another is the backbone of plasmid DNA, associated with the origin

of replication and selection of marker genes, which are necessary for plasmid propagation in bacteria. The level and duration of transgene expression can be regulated by optimization of these plasmid components (Yew, 2005; van Gaal et al., 2006). Figure 1 demonstrates the schematics of the conventional plasmid and the modification of plasmid using various approaches.

#### Promoter/enhancer selection

The promoter is the key region for controlling the profile of transgene expression. Each promoter has a unique transgene expression profile. Therefore, selection of the optimal promoter, including other regulatory elements such as the enhancer, could control the kinetics of the transgene expression pattern of the plasmid. Various types of promoter with different expression characteristics have been reviewed (Yew, 2005). For example, CMV promoter, a widely used promoter that is derived from the regulation region of the immediate early gene of cytomegalovirus (CMV), exhibits transient expression. CMV promoter confers a strong expression of transgene but the level of transgene expression is rapidly reduced. Elongation factor 1  $\alpha$  (EF1 $\alpha$ ) promoter is known to exert sustained gene expression although its expression level is lower than that of CMV promoter. Therefore, optimization of the promoter and enhancer combination is an effective way of obtaining high and sustained gene expression. As a good example of promoter optimization, Magnusson et al. optimized the promoter and enhancer for high and sustained transgene expression. Switching murine CMV (mCMV) enhancer to human CMV (hCMV) enhancer resulted in the sustained expression of luciferase (Luc) activity over 80 days, whereas the Luc expression of mCMV enhancer-driven plasmid DNA fell below the limit of detection in 45 days. This sustained transgene expression achieved with hCMV enhancer might be explained by the differences in type and number of transcription factors between species. Furthermore, to combine the high level of transgene expression from CMV promoter with the sustained expression profile of EF1 $\alpha$  promoter, the shuffle CMV-EF1 $\alpha$  promoter (SCEP) was engineered. The expression profile from SCEP was compared with that of standard promoter, including CMV promoter and EF1 $\alpha$  promoter with hCMV enhancer. CMV promoter showed a very transient expression profile compared with EF1 $\alpha$  promoter and SCEP. Both EF1 $\alpha$  promoter and SCEP showed a similar sustained expression profile. Furthermore, SCEP promoter showed a higher level of transgene expression than EF1 $\alpha$  promoter at all time points. This study demonstrated that a sustained transgene expression can be achieved by optimizing the promoter and enhancer compartment (Magnusson et al., 2011).

#### Modification of plasmid DNA backbone

In addition to the promoter and enhancer, the plasmid DNA backbone should also be considered as it affects the profile of transgene expression.

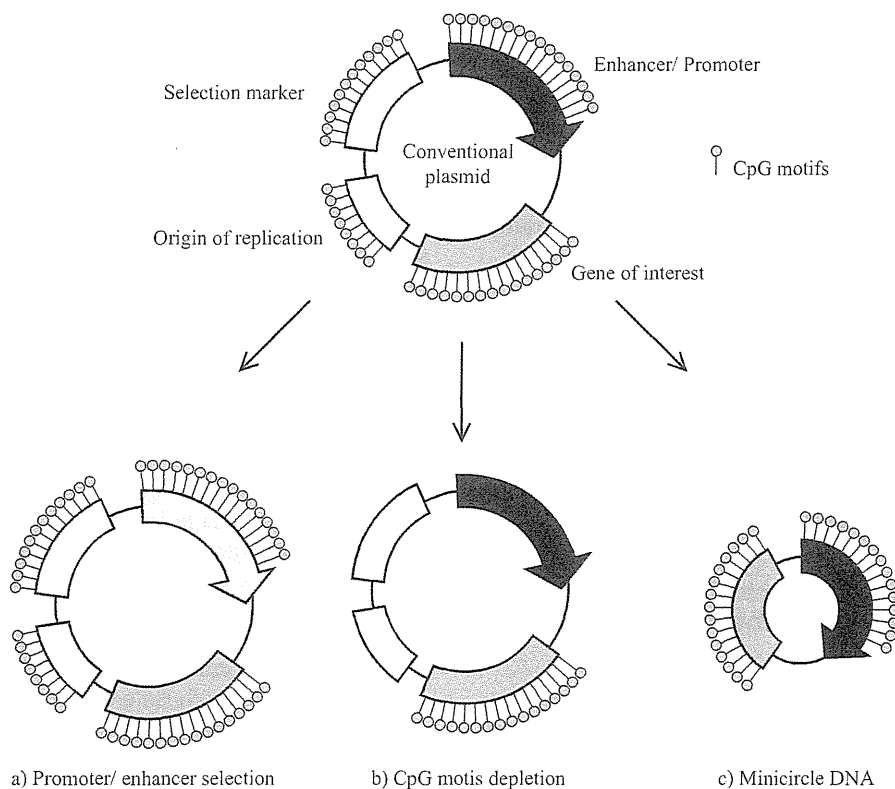


Figure 1. Schematics of conventional (unmodified) plasmid DNA (top image) and the modifications of plasmid DNA for controlling the kinetics of transgene expression: (a) promoter/enhancer selection, (b) depletion of CpG motifs from plasmid DNA and (c) elimination of plasmid bacterial backbone (minicircle DNA).

#### Depletion of CpG-motifs from plasmid DNA

Although plasmid DNA is less immunogenic than viral vectors, the cytosine-phosphate-guanine dinucleotides (CpG motifs) in plasmid DNA can induce inflammatory responses. The recognition of CpG motifs is mediated by Toll-like receptor 9 (TLR9), which consequently results in the generation of pro-inflammatory cytokines, such as tumor necrosis factor (TNF)- $\alpha$  and IFN- $\gamma$ . Generally speaking, these cytokines have negative effects on transgene expression (Scheule, 2000). In addition, the methylation of cytosine residues of the CpG motifs in plasmid DNA may also be related to transgene silencing (Scheule, 2000; Takahashi et al., 2012; Yew & Cheng, 2004). Therefore, the elimination of CpG motifs from plasmid DNA could reduce immune responses to the DNA and transgene silencing, resulting in the prolongation of transgene expression. Yew et al. constructed a plasmid DNA with a reduced number of CpG motifs (Yew et al., 2002). They named this plasmid vector pGZB vector. pGZB coding chloramphenicol acetyltransferase (CAT), pGZB-sCAT (containing 102 CpG motifs), increased the duration of CAT expression in the lung and liver after *in vivo* gene transfer compared with ones consisting of conventional CpG-replete plasmid DNA (256 CpG motifs). Similar results were obtained when the CAT gene was replaced with blood coagulation factor IX. This study supported the hypothesis that persistent transgene

expression is achieved by reducing the number of CpG motifs from plasmid DNA.

#### Minicircle DNA

Minicircle DNA, also known as a supercoiled minimal expression cassette, is an abridged form of conventional plasmid DNA obtained by eliminating all bacterial components, including a replication origin and an anti-bacterial resistant gene. Minicircle DNA contains only an expression cassette including cDNA, enhancer and promoter (Mayrhofer et al., 2009). The initial concept of minicircle DNA is similar to CpG reduced plasmid DNA, namely, to avoid transgene silencing mediated by bacterial-derived sequences. Several studies have reported that more persistent transgene expression is obtained with minicircle DNA compared with their parenteral plasmid DNA (Chen et al., 2003; Wu et al., 2006; Argyros et al., 2011; Huang et al., 2009), even though the mechanism whereby bacterial sequences suppress transgene expression remains unclear. Chen et al. have obtained evidence that silencing of transgene expression was not merely affected by the CpG content or CpG methylation of DNA but was mediated by the covalent linkage of the plasmid backbone to the expression cassette (Chen et al., 2004; Riu et al., 2005). They suggested that the formation of repressive heterochromatin over the plasmid DNA backbone and its ability to spread out to the adjacent

regions might be involved in the transgene silencing (Chen et al., 2004; Chen et al., 2008). Furthermore, the latest report from the same group provided strong evidence that the length but not the sequence of the DNA insert between the 5' and 3' ends of transgene expression cassette is critical for transgene silencing (Lu et al., 2012). Moreover, several pieces of evidence have indicated an inverse correlation between plasmid size and transgene expression efficiency (Kreiss et al., 1999; Yin et al., 2005). Considering these observations, it seems that the reduced number of CpG content is not the main factor responsible for the improved and persistent transgene expression from minicircle DNA over parenteral plasmid DNA. Instead, elimination of the plasmid bacterial backbone, shortening of the spacer between 5' and 3' ends of the transgene expression cassette and a reduction in plasmid size could be the reason for persistent transgene expression from minicircle DNA.

### Rational design of plasmid DNA encoding the IFN gene to control the kinetics of transgene expression

The development of IFN-based therapy has been hindered by the many disadvantages of IFN, such as its short *in vivo* half-life, which requires multiple and frequent administration. These increase patient-noncompliance and the cost. Gene delivery of IFN can be used to overcome these problems. As described above, a rational design of plasmid DNA encoding the IFN gene is effective in optimizing IFN transgene expression. This section reviews the application of the strategies to IFN expressing plasmid DNA.

#### Improved duration of IFN transgene expression by using CpG reduced plasmid DNA

As already described, removal of CpG motifs from plasmid DNA generally results in the prolongation of transgene expression. We have demonstrated that prolonged expression of IFN- $\beta$  and IFN- $\gamma$  was obtained by using CpG reduced pGZB vector. A single hydrodynamic injection of pGZB vector encoding murine IFN- $\beta$  (pGZB-Mu $\beta$ ) into mice resulted in more sustained expression of IFN- $\beta$  compared with CpG-replete pCMV-Mu $\beta$ . Moreover, the inhibitory effect of IFN- $\beta$  gene transfer on pulmonary metastasis of CT-26 carcinoma cells was high in mice receiving pGZB-Mu $\beta$  compared with that in those receiving pCMV-Mu $\beta$ . Similar results were obtained with plasmids expressing murine IFN- $\gamma$ . These results indicate that the removal of CpG motifs from plasmid DNA enhances the therapeutic effects of IFN gene transfer through prolongation of IFN transgene expression (Kawano et al., 2007). In order to further reduce the number of CpG motifs in plasmid DNA, CpG-free plasmid vector, called pCpG plasmid (Invivogen), which has no CpG motifs, was chosen to construct plasmid DNA encoding murine IFN- $\gamma$  (pCpG-Mu $\gamma$ ). As expected, administration of pCpG-Mu $\gamma$  resulted in more sustained

IFN- $\gamma$  expression and a greater anti-tumor effect compared with that of pGZB-Mu $\gamma$  or pCMV-Mu $\gamma$  (Mitsui et al., 2009). The sustained expression of IFN- $\gamma$  from pCpG-Mu $\gamma$  was also beneficial in treating chronic diseases, like atopic dermatitis. We succeeded in ameliorating the development of Th2 dominant atopic dermatitis in NC/Nga mice, a mouse model of atopic dermatitis (Hattori et al., 2010). The sustained IFN- $\gamma$  expression in mice shifted the immunological balance toward Th1. This effect was not observed in mice receiving multiple injections of pCMV-Mu $\gamma$ . Therefore, we proposed CpG depleted plasmid DNA encoding IFN- $\gamma$ , pCpG-Mu $\gamma$  as a useful method for IFN- $\gamma$  gene therapy.

#### Combination of CpG reduction and selection of promoter/enhancer

CpG reduced plasmid DNA encoding murine IFN- $\gamma$  provided high and sustained transgene expression of IFN- $\gamma$  in mice after hydrodynamic injection and produced potent therapeutic effects on tumor growth or atopic dermatitis (Mitsui et al., 2009; Hattori et al., 2010). However, the administration of pCpG-Mu $\gamma$  was associated with very high concentrations of IFN- $\gamma$  soon after gene transfer, which fell with time to a constant, steady level. The high initial concentrations of IFN $\gamma$  could induce unwanted responses, such as body weight loss. The plasmid pCpG-Mu $\gamma$  contains human elongation factor (hEF)-1 promoter and murine cytomegalovirus (mCMV) enhancer. The hydrodynamic injection method, which was used for gene transfer in the study of plasmid pCpG-Mu $\gamma$ , has been reported to activate transcription factors, including activator protein (AP)-1 and nuclear factor (NF)- $\kappa$ B in the liver (Nishikawa et al., 2008). As mCMV enhancer contains many binding sites for AP-1 and NF- $\kappa$ B, the activation of transcription factors by hydrodynamic injection could result in an initial surge in transgene expression. We designed and constructed a plasmid vector that exhibits a constant and steady expression of IFN- $\gamma$  for minimizing the adverse effects caused by initial high concentrations of IFN- $\gamma$  (Ando et al., 2012). As the kinetics of transgene expression is mainly governed by the type of promoter and enhancer, we constructed a series of plasmid vectors with different promoters and enhancers. As a result, we found that the plasmid DNA containing human ROSA26 (hROSA26) promoter produced a constant and steady expression of IFN- $\gamma$ . Furthermore, adverse effects, such as body weight loss, which was observed in mice receiving a high dose pCpG-Mu $\gamma$ , were not observed in mice receiving hROSA promoter-driven IFN $\gamma$ -expressing plasmid DNA. Lack of binding sites for AP-1 and NF- $\kappa$ B in the hROSA26 promoter seems to be responsible for the constant transgene expression. Interestingly, the duration of IFN- $\gamma$  transgene expression from hROSA26 promoter-containing plasmid DNA was comparable with that from pCpG plasmid, despite the fact that the hROSA26 promoter contains as many as 428 CpG motifs. As the hROSA26 promoter contains many binding sites for SP1, a steady transcription

factor, sustained transgene expression from hROSA26 promoter might be due to its many SP-1 binding sites. The reason why sustained transgene expression is obtained by using the CpG replete hROSA26 promoter-driven plasmid DNA has not been identified yet. However, these results suggest that the number of CpG motifs in plasmid DNA is not a major factor controlling the profile of transgene expression.

#### Minicircle DNA with a tumor-selective promoter as a tumor-specific expression system

Minicircle DNA is attractive for persistent transgene expression. Wu et al. applied this DNA to IFN- $\gamma$  gene therapy of cancer. The anti-tumor effects of IFN- $\gamma$  on human nasopharyngeal carcinoma (NPC) were studied by using minicircle-mediated IFN- $\gamma$  gene transfer. IFN- $\gamma$  gene transfer by minicircle DNA exhibited better antiproliferative effects in NPC tumor-bearing mice than those obtained by its plasmid DNA counterpart, which was a consequence of a high and persistent transgene expression of IFN- $\gamma$  from the minicircle DNA (Wu et al., 2006). As a close correlation between the pathogenesis of NPC and EBV infection has been reported (Raab-Traub, 2002), oriP promoter, which contains many binding sites for EBV nuclear antigen 1 (EBNA-1), was used for minicircle DNA encoding IFN- $\gamma$  to increase the specificity of transgene expression in NPC tumors (Yates et al., 2000). The results obtained showed that minicircle DNA, the IFN- $\gamma$  expression of which was driven by the oriP promoter, had no anti-tumor effects on EBV-negative tumor xenografts but produced tumor regression and prolonged survival in EBV positive tumor-bearing mice. Moreover, the IFN- $\gamma$  level in the liver was significantly lower in mice receiving oriP promoter-based minicircle DNA than that in those receiving CMV promoter-based minicircle DNA. These findings suggest that the oriP promoter-based IFN- $\gamma$ -expressing minicircle DNA can be used as a safe and effective therapy to treat EBV positive NPC (Zuo et al., 2011).

#### Small molecule-inducible plasmid DNA for long-term and renewable transgene expression

Drug-regulated transgene expression systems have been established to manipulate spatial and temporal aspects of transgene expression. Generally, this plasmid system consists of two key components. The first component expresses an inactive form of a regulatory protein, which will be activated after binding of a small-molecule inducer. The other one carries the transgene of interest, which is expressed in response to the activation of the regulatory protein (Nordstrom, 2003). A mifepristone (MFP)-inducible plasmid system, termed pBRES has been constructed by Szymanski et al. A variety of transgenes, including human IFN $\beta$ , were inserted into the pBRES plasmid and the regulation of transgene expression in response to MFP was examined. For example, the intraperitoneal injection of MFP following the transfection of pBRES plasmid encoding human IFN $\beta$

(pBRES-hIFN $\beta$ ) into murine hind limb muscles with electroporation resulted in detectable serum levels of hIFN $\beta$  while, in the absence of MFP, the level of hIFN $\beta$  in mouse serum was undetectable (Szymanski et al., 2007). Harkins et al. applied the pBRES plasmid system for encoding murine IFN- $\beta$  and investigated the therapeutic effect in a murine model of experimental allergic encephalomyelitis (EAE). This plasmid DNA induced efficient and sustained expression of interferon-inducible protein-10, which is used as a marker of IFN activity, in mice for up to 3 months under MFP induction. Repeated administration of plasmid resulted in renewed expression. The administration of the pBRES murine IFN $\beta$  plasmid with an inducer MFP produced an efficient therapeutic effect compared with the control plasmid or pBRES murine IFN- $\beta$  plasmid administration without MFP in a mouse model of EAE (Harkins et al., 2008).

#### Conclusions

IFN gene transfer could avoid the many drawbacks of IFN-based therapy and a number of clinical trials have been conducted using IFN gene transfer (Kalanjeri & Stermann, 2012). However, most of these studies use viral vectors. Only few studies were conducted using non-viral vectors like cationic liposomes (Matsumoto et al., 2008; Wakabayashi et al., 2008). In order to expand the range of IFN gene therapy by plasmid DNA vector, an engineered plasmid DNA vector that can regulate spatio-temporal distribution of IFN is required. In the present review, we have summarized attractive strategies that can be used to obtain more precisely controlled transgene expression of IFN from modified plasmid DNA, which could be applied via simple administration methods, such as hydrodynamic injection (Ando et al., 2012; Hattori et al., 2010; Mitsui et al., 2009), intramuscular injection (Harkins et al., 2008), and intratumoral injection of plasmid DNA/cationic liposome complex (Wu et al., 2006; Zuo et al., 2011). Using plasmid modification techniques described in the present review is a promising strategy for improving the therapeutic efficacy and safety profile of IFN gene therapy.

#### Declaration of interest

The authors report no conflicts of interest.

#### References

- Ando M, Takahashi Y, Nishikawa M, Watanabe Y, Takakura Y. (2012). Constant and steady transgene expression of interferon- $\gamma$  by optimization of plasmid construct for safe and effective interferon- $\gamma$  gene therapy. *J Gene Med*, 14, 288–295.
- Argyros O, Wong SP, Fedonidis C, Tolmachov O, Waddington SN, Howe SJ, Niceta M, Coutelle C, Harbottle RP. (2011). Development of S/MAR minicircles for enhanced and persistent transgene expression in the mouse liver. *J Mol Med*, 89, 515–529.
- Bracarda S, Eggermont AM, Samuelsson J. (2010). Redefining the role of interferon in the treatment of malignant diseases. *Eur J Cancer*, 46, 284–297.

- Chen ZY, He CY, Ehrhardt A, Kay MA. (2003). Minicircle DNA vectors devoid of bacterial DNA result in persistent and high-level transgene expression *in vivo*. *Mol Ther*, 8, 495–500.
- Chen ZY, He CY, Meuse L, Kay MA. (2004). Silencing of episomal transgene expression by plasmid bacterial DNA elements *in vivo*. *Gene Ther*, 11, 856–864.
- Chen ZY, Riu E, He CY, Xu H, Kay MA. (2008). Silencing of episomal transgene expression in liver by plasmid bacterial backbone DNA is independent of CpG methylation. *Mol Ther*, 16, 548–556.
- Edelstein M. (2012). Gene therapy clinical trials worldwide [Online]. John Wiley and Sons Ltd. Available: <http://www.wiley.com/legacy/wileychi/genmed/clinical/> [Accessed 24 April 2012].
- Edelstein ML, Abedi MR, Wixon J. (2007). Gene therapy clinical trials worldwide to 2007—an update. *J Gene Med*, 9, 833–842.
- Edelstein ML, Abedi MR, Wixon J, Edelstein RM. (2004). Gene therapy clinical trials worldwide 1989–2004—an overview. *J Gene Med*, 6, 597–602.
- Harkins RN, Szymanski P, Petry H, Brooks A, Qian HS, Schaefer C, Kretschmer PJ, Orme A, Wang P, Rubanyi GM, Hermiston TW. (2008). Regulated expression of the interferon-beta gene in mice. *Gene Ther*, 15, 1–11.
- Hattori K, Nishikawa M, Watcharanurak K, Ikoma A, Kabashima K, Toyota H, Takahashi Y, Takahashi R, Watanabe Y, Takakura Y. (2010). Sustained exogenous expression of therapeutic levels of IFN-gamma ameliorates atopic dermatitis in NC/Nga mice via Th1 polarization. *J Immunol*, 184, 2729–2735.
- Huang M, Chen Z, Hu S, Jia F, Li Z, Hoyt G, Robbins RC, Kay MA, Wu JC. (2009). Novel minicircle vector for gene therapy in murine myocardial infarction. *Circulation*, 120, S230–S237.
- Kalanjeri S, Serman D. (2012). Gene therapy in interventional pulmonology: Interferon gene delivery with focus on thoracic malignancies. *Curr Resp Care Rep*, 1, 54–66.
- Kamimura K, Suda T, Zhang G, Liu D. (2011). *Advances in Gene Delivery Systems*. *Pharmaceut Med*, 25, 293–306.
- Kawano H, Nishikawa M, Mitsui M, Takahashi Y, Kako K, Yamaoka K, Watanabe Y, Takakura Y. (2007). Improved anti-cancer effect of interferon gene transfer by sustained expression using CpG-reduced plasmid DNA. *Int J Cancer*, 121, 401–406.
- Kreiss P, Cameron B, Rangara R, Mailhe P, Aguerre-Charriol O, Airiau M, Scherman D, Crouzet J, Pitard B. (1999). Plasmid DNA size does not affect the physicochemical properties of lipoplexes but modulates gene transfer efficiency. *Nucleic Acids Res*, 27, 3792–3798.
- Lu J, Zhang F, Xu S, Fire AZ, Kay MA. (2012). The extragenic spacer length between the 5' and 3' ends of the transgene expression cassette affects transgene silencing from plasmid-based vectors. *Mol Ther*. DOI: 10.1038/mt.2012.65.
- Magnusson T, Haase R, Schleaf M, Wagner E, Ogris M. (2011). Sustained, high transgene expression in liver with plasmid vectors using optimized promoter-enhancer combinations. *J Gene Med*, 13, 382–391.
- Matsumoto K, Kubo H, Murata H, Uhara H, Takata M, Shibata S, Yasue S, Sakakibara A, Tomita Y, Kageshita T, Kawakami Y, Mizuno M, Yoshida J, Saida T. (2008). A pilot study of human interferon beta gene therapy for patients with advanced melanoma by *in vivo* transduction using cationic liposomes. *Jpn J Clin Oncol*, 38, 849–856.
- Mayrhofer P, Schleaf M, Jechlinger W. (2009). Use of minicircle plasmids for gene therapy. *Methods Mol Biol*, 542, 87–104.
- Mehier-Humbert S, Guy RH. (2005). Physical methods for gene transfer: improving the kinetics of gene delivery into cells. *Adv Drug Deliv Rev*, 57, 733–753.
- Mitsui M, Nishikawa M, Zang L, Ando M, Hattori K, Takahashi Y, Watanabe Y, Takakura Y. (2009). Effect of the content of unmethylated CpG dinucleotides in plasmid DNA on the sustainability of transgene expression. *J Gene Med*, 11, 435–443.
- Nishikawa M, Hashida M. (2002). Nonviral approaches satisfying various requirements for effective *in vivo* gene therapy. *Biol Pharm Bull*, 25, 275–283.
- Nishikawa M, Huang L. (2001). Nonviral vectors in the new millennium: delivery barriers in gene transfer. *Hum Gene Ther*, 12, 861–870.
- Nishikawa M, Nakayama A, Takahashi Y, Fukuhara Y, Takakura Y. (2008). Reactivation of silenced transgene expression in mouse liver by rapid, large-volume injection of isotonic solution. *Hum Gene Ther*, 19, 1009–1020.
- Nordstrom JL. (2003). The antiprogesterone-dependent GeneSwitch system for regulated gene therapy. *Steroids*, 68, 1085–1094.
- Platanias LC. (2005). Mechanisms of type-I- and type-II-interferon-mediated signalling. *Nat Rev Immunol*, 5, 375–386.
- Raab-Traub N. (2002). Epstein-Barr virus in the pathogenesis of NPC. *Semin Cancer Biol*, 12, 431–441.
- Riu E, Grimm D, Huang Z, Kay MA. (2005). Increased maintenance and persistence of transgenes by excision of expression cassettes from plasmid sequences *in vivo*. *Hum Gene Ther*, 16, 558–570.
- Sadler AJ, Williams BR. (2008). Interferon-inducible antiviral effectors. *Nat Rev Immunol*, 8, 559–568.
- Scheule RK. (2000). The role of CpG motifs in immunostimulation and gene therapy. *Adv Drug Deliv Rev*, 44, 119–134.
- Szymanski P, Kretschmer PJ, Bauzon M, Jin F, Qian HS, Rubanyi GM, Harkins RN, Hermiston TW. (2007). Development and validation of a robust and versatile one-plasmid regulated gene expression system. *Mol Ther*, 15, 1340–1347.
- Takahashi Y, Nishikawa M, Takakura Y. (2012). Development of safe and effective nonviral gene therapy by eliminating CpG motifs from plasmid DNA vector. *Front Biosci (Schol Ed)*, 4, 133–141.
- van Gaal EV, Hennink WE, Crommelin DJ, Mastrobattista E. (2006). Plasmid engineering for controlled and sustained gene expression for nonviral gene therapy. *Pharm Res*, 23, 1053–1074.
- Wakabayashi T, Natsume A, Hashizume Y, Fujii M, Mizuno M, Yoshida J. (2008). A phase I clinical trial of interferon-beta gene therapy for high-grade glioma: novel findings from gene expression profiling and autopsy. *J Gene Med*, 10, 329–339.
- Wu J, Xiao X, Zhao P, Xue G, Zhu Y, Zhu X, Zheng L, Zeng Y, Huang W. (2006). Minicircle-IFN $\gamma$  induces antiproliferative and antitumoral effects in human nasopharyngeal carcinoma. *Clin Cancer Res*, 12, 4702–4713.
- Yates JL, Camiolo SM, Bashaw JM. (2000). The minimal replicator of Epstein-Barr virus oriP. *J Virol*, 74, 4512–4522.
- Yew NS. (2005). Controlling the kinetics of transgene expression by plasmid design. *Adv Drug Deliv Rev*, 57, 769–780.
- Yew NS, Cheng SH. (2004). Reducing the immunostimulatory activity of CpG-containing plasmid DNA vectors for non-viral gene therapy. *Expert Opin Drug Deliv*, 1, 115–125.
- Yew NS, Zhao H, Przybylska M, Wu IH, Tousignant JD, Scheule RK, Cheng SH. (2002). CpG-depleted plasmid DNA vectors with enhanced safety and long-term gene expression *in vivo*. *Mol Ther*, 5, 731–738.
- Yin W, Xiang P, Li Q. (2005). Investigations of the effect of DNA size in transient transfection assay using dual luciferase system. *Anal Biochem*, 346, 289–294.
- Zuo Y, Wu J, Xu Z, Yang S, Yan H, Tan L, Meng X, Ying X, Liu R, Kang T, Huang W. (2011). Minicircle-oriP-IFN $\gamma$ : a novel targeted gene therapeutic system for EBV positive human nasopharyngeal carcinoma. *PLoS ONE*, 6, e19407.

## RESEARCH ARTICLE

# Gene Delivery of Albumin Binding Peptide-Interferon-gamma Fusion Protein with Improved Pharmacokinetic Properties and Sustained Biological Activity

NORIKO MIYAKAWA,<sup>1</sup> MAKIYA NISHIKAWA,<sup>1</sup> YUKI TAKAHASHI,<sup>1</sup> MITSURU ANDO,<sup>1</sup> MASAYUKI MISAKA,<sup>1</sup> YOSHIHIKO WATANABE,<sup>2</sup> YOSHINOBU TAKAKURA<sup>1</sup>

<sup>1</sup>Department of Biopharmaceutics and Drug Metabolism, Graduate School of Pharmaceutical Science, Kyoto University, Kyoto 606-8501, Japan

<sup>2</sup>Department of Molecular Microbiology, Graduate School of Pharmaceutical Science, Kyoto University, Kyoto 606-8501, Japan

Received 7 November 2012; revised 31 January 2013; accepted 12 February 2013

Published online in Wiley Online Library (wileyonlinelibrary.com). DOI 10.1002/jps.23493

**ABSTRACT:** We have demonstrated that gene delivery of a fusion protein of mouse interferon (IFN)  $\gamma$  with mouse serum albumin (IFN $\gamma$ -MSA) was effective in prolonging the circulation half-life of IFN $\gamma$  in mice. However, the fusion to MSA greatly reduced the biological activity of IFN $\gamma$  to less than 1%. In this study, we designed IFN $\gamma$  fusion proteins with a 20 amino-acid long albumin-binding peptide (ABP) to prolong the *in vivo* half-life of IFN $\gamma$  without reducing its biological activity. IFN $\gamma$ -ABP and ABP-IFN $\gamma$ , two fusion proteins with the ABP being fused to the C- or N-terminal of IFN $\gamma$ , retained 40%–50% biological activities determined using a gamma-activated sequence-dependent luciferase assay. These fusion proteins exhibited the ability to bind to MSA. Gene delivery of IFN $\gamma$ -ABP or ABP-IFN $\gamma$  to mice using the hydrodynamic injection method resulted in a sustained concentration of IFN $\gamma$  in the serum compared with gene delivery of IFN $\gamma$ . In addition, the growth of mouse colon carcinoma CT-26 cells in the lung was efficiently inhibited by gene delivery of the IFN $\gamma$  fusion proteins. These results indicate that the fusion of ABP is a useful approach to achieving prolonged retention in the blood circulation through binding to serum albumin and retaining biological activity. © 2013 Wiley Periodicals, Inc. and the American Pharmacists Association *J Pharm Sci*

**Keywords:** albumin; albumin-binding peptide; biological activity; clearance; fusion protein; gene delivery; hydrodynamic injection; moment analysis; plasmid DNA; pharmacokinetics

## INTRODUCTION

Interferon-gamma (IFN $\gamma$ ) is a pleiotropic cytokine with antiviral, antiproliferative, and immunomodulatory activities.<sup>1,2</sup> Despite extensive studies in the last two decades, the clinical application of IFN $\gamma$  is limited to the treatment of a small number of diseases, including chronic granulomatous disease, osteopetrosis, and renal cancer, largely because of its short *in vivo* half-life.<sup>2–4</sup> Frequent injections are required to maintain effective concentrations, but the fluctuating blood concentration of IFN $\gamma$  produced by frequent dosing leads to serious adverse toxic effects, including fever, fatigue, and neurotoxicity.<sup>2,5,6</sup>

Gene delivery of a therapeutic protein with unsatisfactory pharmacokinetic properties, such as a short *in vivo* half-life, is a promising approach to achieving sustained therapeutic effects with minimal toxicity. In previous studies, we showed that plasmid-based gene delivery of IFN $\gamma$  is effective in inhibiting metastatic tumor growth and atopic dermatitis in mice.<sup>7–10</sup> These studies indicated the therapeutic potential of IFN $\gamma$  gene transfer in several disease models. However, we also found that high doses of IFN $\gamma$ -expressing plasmids, especially those expressing IFN $\gamma$  for a long period, induced toxic effects. We hypothesized that controlling the tissue distribution of IFN $\gamma$  expressed from plasmid vectors would be a promising method of reducing such toxic effects. On the basis of this hypothesis, we designed fusion proteins of IFN $\gamma$  with mouse serum albumin (MSA) and constructed plasmids encoding the fusion protein,

Correspondence to: Makiya Nishikawa (Telephone: +81-75-753-4580; Fax: +81-75-753-4614; E-mail: makiya@pharm.kyoto-u.ac.jp)

*Journal of Pharmaceutical Sciences*

© 2013 Wiley Periodicals, Inc. and the American Pharmacists Association



IFN $\gamma$ -MSA.<sup>11</sup> The fusion to MSA resulted in prolongation of the mean residence time of IFN $\gamma$  after gene delivery. However, the fusion also greatly reduced the biological activity of IFN $\gamma$  and the IFN $\gamma$ -MSA exhibited only about 1/200th of the activity of IFN $\gamma$ .

Marked reduction in the biological activity produced by the fusion of MSA would be due to steric hindrance of the IFN $\gamma$ -IFN $\gamma$  receptor interaction by MSA because MSA has a molecular weight of 67,000.<sup>12</sup> Dennis et al.<sup>13-15</sup> reported that the conjugation of a phage-derived 20 amino-acid long albumin-binding peptide (ABP) gave IgG fragments high affinity for serum albumin, leading to an increased *in vivo* circulation half-life.<sup>13-15</sup> The low-molecular weight of the ABP, as well as the noncovalent binding to serum albumin, could prevent it from reducing the biological activity of IFN $\gamma$ .

Here, we designed fusion proteins of IFN $\gamma$  with ABP to increase the half-life of IFN $\gamma$  without any marked reduction in its biological activity. ABP was fused to either the N- or C-terminal end of IFN $\gamma$  with a short linker peptide. We constructed plasmid vectors encoding these fusion proteins and examined their biological activity and binding to serum albumin, and their serum levels after gene transfer in mice. Then, the therapeutic effects of gene delivery of IFN $\gamma$  fusion protein were examined in mice with pulmonary metastases of colon carcinoma cells.

## MATERIALS AND METHODS

### Cell Culture and Animals

An African green monkey kidney fibroblast cell line, COS-7, was obtained from American Type Culture Collection (Manassas, Virginia). A murine melanoma cell line, B16-BL6, was obtained from the Cancer Chemotherapy Center of the Japanese Foundation for Cancer Research (Tokyo, Japan). B16-BL6 and COS-7 cells were cultured in Dulbecco's modified Eagle's medium supplemented with 10% heat-inactivated fetal bovine serum and penicillin-streptomycin-L-glutamine at 37°C. CT-26 cells were cultured in RPMI1640 medium supplemented with 10% heat-inactivated fetal bovine serum and penicillin-streptomycin-L-glutamine at 37°C. Four-week-old male ICR mice and BALB/c mice, approximately 20 g in weight, were purchased from Japan SLC, Inc. (Shizuoka, Japan), and maintained on a standard food and water diet under conventional housing conditions. All animal experiments were approved by the Institutional Animal Experimentation Committee.

### Plasmid DNA

pcDNA3.1 was purchased from Invitrogen (Carlsbad, California). pHRL-thymidine kinase (TK), a renilla

luciferase-expressing plasmid under the control of herpes simplex virus TK promoter, was purchased from Promega (Madison, Wisconsin). pGAS-Luc, a firefly luciferase-expressing plasmid under the control of gamma-activated sequence (GAS) promoter, has been described previously.<sup>11,16</sup> pCMV-IFN $\gamma$ , an IFN $\gamma$ -expressing plasmid under the control of cytomegalovirus (CMV) promoter, has also been described previously.<sup>11</sup> pCMV-IFN $\gamma$ -ABP and pCMV-ABP-IFN $\gamma$ , a plasmid encoding IFN $\gamma$ -ABP (ABP was fused to the C-terminal of IFN $\gamma$ ) or ABP-IFN $\gamma$  (ABP was fused to the N-terminal), respectively, were constructed by the following method. An IFN $\gamma$ -ABP or ABP-IFN $\gamma$  cDNA fragment was amplified by polymerase chain reaction (PCR) from pCMV-IFN $\gamma$  using a primer with the addition of ABP sequences (GRLMEDICIPRWGCLWEDDF)<sup>14</sup> to the C- or N-terminal of IFN $\gamma$ . Oligonucleotides encoding a 4 amino-acid (GGGS) linker were inserted between IFN $\gamma$  cDNA and ABP sequences according to a previous report.<sup>14,17</sup> The fragment was then inserted into the BamHI/XbaI sites of pcDNA3.1. Each plasmid was amplified in *Escherichia coli* (DH5 $\alpha$ , TOYOBO, Osaka, Japan) and purified using a JETSTAR plasmid purification kit (GENOMED, Löhne, Germany).

### In Vitro Transfection

Cells were seeded on 10 cm dishes at a density of  $1 \times 10^6$  cells/dish or 12-well culture plates at  $1 \times 10^5$  cells/well and incubated overnight and the cells were transfected with the indicated plasmid using Lipofectamine2000 (Invitrogen) according to the manufacturer's instructions. In brief, 1  $\mu$ g plasmid was mixed with 3  $\mu$ L Lipofectamine2000 in Opti-MEM (Invitrogen) at a final concentration of 2  $\mu$ g DNA/mL and the complex obtained was added to cells. The total amount of plasmid DNA used for transfection was 8  $\mu$ g/dish for 10 cm dishes and 1  $\mu$ g/well for 12-well culture plates, respectively.

### Collection of Conditioned Medium

COS-7 cells seeded on 10-cm dishes were transfected with pCMV-IFN $\gamma$ , pCMV-IFN $\gamma$ -ABP, or pCMV-ABP-IFN $\gamma$  as described above. Four hour after transfection, cells were washed with PBS and cultured with serum-free Opti-MEM medium for 48 h. Then, the culture medium was collected as conditioned medium.

### Western Blotting

The conditioned medium of COS-7 cells transfected with pCMV-IFN $\gamma$ , pCMV-IFN $\gamma$ -ABP, or pCMV-ABP-IFN $\gamma$  were collected as described above. The samples were reduced by the addition of dithiothreitol (0.1 M) and heat treatment at 95°C for 4 min to disrupt the disulfide bonds and to dissociate any homodimers that might be present. The samples were



then applied onto 12.5% polyacrylamide gel and were electrophoresed in the presence of sodium dodecyl sulfate (SDS) at the voltage of 200 V for 40 min. After SDS-polyacrylamide gel electrophoresis (PAGE), proteins resolved in the gel were electrophoretically transferred to a PVDF membrane using a wet blotting method in a buffer containing 25 mM Tris, 192 mM glycine, and 20% methanol at the voltage of 200 V for 45 min. After blocking with 5% skimmed milk, the membrane was probed with goat antimouse IFN $\gamma$  polyclonal antibody (R&D System, Inc., Minneapolis, Minnesota) overnight at 4°C and then allowed to react with antigoat IgG antibody conjugated with horseradish peroxidase (Santa Cruz, Inc., Santa Cruz, California) for 1 h at room temperature. The bands were detected with LAS-3000 (Fuji Film, Tokyo, Japan).

#### Measurement of the Biological Activity of IFN $\gamma$ , IFN $\gamma$ -ABP, and ABP-IFN $\gamma$

B16-BL6 cells were cotransfected with pGAS-Luc (1.4  $\mu$ g/mL) and phRL-TK (0.6  $\mu$ g/mL). After a 4 h transfection, the culture medium was replaced with fresh serum-free Opti-MEM containing serial dilutions of the conditioned medium of COS-7 cells transfected with pCMV-IFN $\gamma$ , pCMV-IFN $\gamma$ -ABP, or pCMV-ABP-IFN $\gamma$ . After a 24 h incubation, cells were lysed with a lysis buffer (0.1 M Tris, 0.05% Triton-X-100, 2 mM ethylenediaminetetraacetic acid, pH 7.8) and the lysates were mixed with reagents of the Dual-Luciferase Reporter Assay System (Promega). Then, firefly and renilla luciferase activity was measured in a luminometer (Lumat LB 9507; EG&G Bethhold, Bad Wildbad, Germany) and the ratio of firefly luciferase activity to renilla luciferase activity was calculated. Here, firefly luciferase activity was used as an indicator of IFN $\gamma$ -driven transcription and renilla luciferase activity was used for normalization of the transfection efficiency and cell number.<sup>18</sup> The firefly/renilla ratio of the cells treated with indicated concentrations of IFN $\gamma$ , IFN $\gamma$ -ABP, or ABP-IFN $\gamma$  was divided by the firefly/renilla ratio of the cells cultured without IFN $\gamma$ , IFN $\gamma$ -ABP, or ABP-IFN $\gamma$  to give fold increase in GAS-dependent luciferase activity relative to those of the untreated group. Finally, the half maximum effective concentration (EC50) of IFN $\gamma$ , IFN $\gamma$ -ABP, and ABP-IFN $\gamma$  was calculated. In a separate set of experiments, 100 pg/mL of IFN $\gamma$ , IFN $\gamma$ -ABP, or ABP-IFN $\gamma$  was incubated with or without 0.25 mg/mL of MSA (Sigma; St. Louis, MO, USA) in Opti-MEM at 37°C for 1 h, and added to B16-BL6 cells transfected with pGAS-Luc and phRL-TK. Then, the fold increase in GAS-dependent luciferase activity relative to that of the untreated group was calculated as described above.

#### Measurement of the Binding Affinity of IFN $\gamma$ , IFN $\gamma$ -ABP, and ABP-IFN $\gamma$ for MSA

Mouse serum albumin was immobilized onto 96-well plates at a concentration of 2  $\mu$ g/mL overnight at 4°C. Wells were added with serially diluted supernatants of COS-7 cells transfected with pCMV-IFN $\gamma$ , pCMV-IFN $\gamma$ -ABP, or pCMV-ABP-IFN $\gamma$ . After incubation for 2 h at room temperature, each well was washed with phosphate buffered saline-0.05% Tween 20 and proteins bound to MSA were detected by enzyme-linked immunosorbent assay (ELISA) using antimouse IFN $\gamma$  antibody (eBioscience, San Diego, California).<sup>13,14</sup>

#### *In Vivo* Gene Transfer

For gene transfer to mouse liver, mice received a hydrodynamic injection via the tail vein of plasmid DNA dissolved in 1.6 mL saline within 5 s.<sup>19,20</sup> The dose of plasmids was set at 0.2 pmol/mouse based on preliminary experiments. At predetermined periods, blood was collected from the tail vein and the blood samples were kept at 4°C for 2 h and centrifuged at 8000g for 20 min to obtain serum.

#### Measurement of mRNA Expression of IFN $\gamma$ , IFN $\gamma$ -ABP, and ABP-IFN $\gamma$ in the Liver

Six hours after gene transfer, mice were sacrificed and total RNA was extracted from approximately 50 mg liver samples using Sepasol RNA I Super (Nacalai Tesque, Kyoto, Japan). After removal of contaminated DNA by DNase I (Takara Bio, Shiga, Japan), reverse transcription was performed using a ReverTra Ace qPCR RT kit (TOYOBO), followed by RNaseH treatment (Ribonuclease H; Takara Bio). For a quantitative analysis of mRNA expression, a real-time PCR was carried out with total cDNA using KAPA SYBR FAST ABI Prism 2 $\times$  qPCR Master Mix (KAPA BIOSYSTEMS, Boston, Massachusetts). The oligonucleotide primers used for amplification were: *Ifn $\gamma$* -sense: 5'-CGGCACAGTCATTGAAAGCCTA-3', *Ifn $\gamma$* -antisense: 5'-GTTGCTGATGGCCTGATTGTC-3', and  $\beta$ -actin-sense: 5'-CATCCGTAAGACCTCTATGC-3',  $\beta$ -actin-antisense: 5'-ATGGAGCCACCGATCCACA-3. Amplified products were detected via intercalation of the fluorescent dye using a StepOnePlus Real Time PCR System (Applied Biosystems, Foster City, California). The mRNA expression of IFN $\gamma$  was normalized using the mRNA level of  $\beta$ -actin.

#### Measurement of the Concentrations of IFN $\gamma$ , IFN $\gamma$ -ABP, and ABP-IFN $\gamma$

The concentrations of IFN $\gamma$ , IFN $\gamma$ -ABP, and ABP-IFN $\gamma$  in the supernatant of COS-7 cells or mouse serum were determined by ELISA using a

commercial kit (Ready-SET-Go! MuIFN- $\gamma$  ELISA; eBioscience).

#### Clearance of IFN $\gamma$ , IFN $\gamma$ -ABP, and ABP-IFN $\gamma$ after Intravenous Injection into Mice

To obtain IFN $\gamma$ , IFN $\gamma$ -ABP, and ABP-IFN $\gamma$  proteins, mice received a hydrodynamic injection of pCMV-IFN $\gamma$ , pCMV-IFN $\gamma$ -ABP, or pCMV-ABP-IFN $\gamma$  as described above at a dose of 5 pmol/mouse. At 12 h after injection, blood was collected from the inferior vena cava and the serum was obtained in the same manner as described above. The serum samples containing IFN $\gamma$ , IFN $\gamma$ -ABP, or ABP-IFN $\gamma$  were injected into different mice via the tail vein and blood was periodically sampled. The dose of each protein was set at 8.5  $\mu$ g IFN $\gamma$ /kg, and this was quantified by ELISA.<sup>11</sup>

#### Experimental Metastatic Pulmonary Tumor Model

CT-26 cells were trypsinized and suspended in Hanks' balanced salt solution (HBSS). Cell suspensions containing  $1 \times 10^5$  CT-26 cells in 200  $\mu$ L HBSS were injected into the tail vein of syngeneic BALB/c mice to establish an experimental metastatic pulmonary tumor model. Then, 3 days after inoculation of the CT-26 cells, each plasmid was injected into the tail vein by the hydrodynamic injection method at a dose of 0.7 pmol/mouse. At 14 days after inoculation, mice were sacrificed and the lungs were collected. The lungs were immersed in 100% methanol to make metastatic colonies more visible. Then, the number of metastatic colonies on the lung surface was counted by the naked eye.<sup>11,21</sup>

#### Pharmacokinetic Analysis

The peak plasma concentrations ( $C_{max}$ ) and the time of maximum serum concentration ( $t_{max}$ ) were obtained from actual data recorded after injection or gene transfer. The area under the serum concentration-time curve (AUC) and mean retention time (MRT) were calculated using a moment analysis method. These parameters were calculated for each animal by integration to infinite time.<sup>22</sup>

#### Data Analysis

Differences were statistically evaluated by Student's *t*-test, and the level of statistical significance was set at  $p < 0.05$ .

## RESULTS

#### Expression of IFN $\gamma$ -ABP and ABP-IFN $\gamma$ in Cultured Cells

Figure 1a shows the Western blot analysis of the expression of IFN $\gamma$ , IFN $\gamma$ -ABP, and ABP-IFN $\gamma$  in

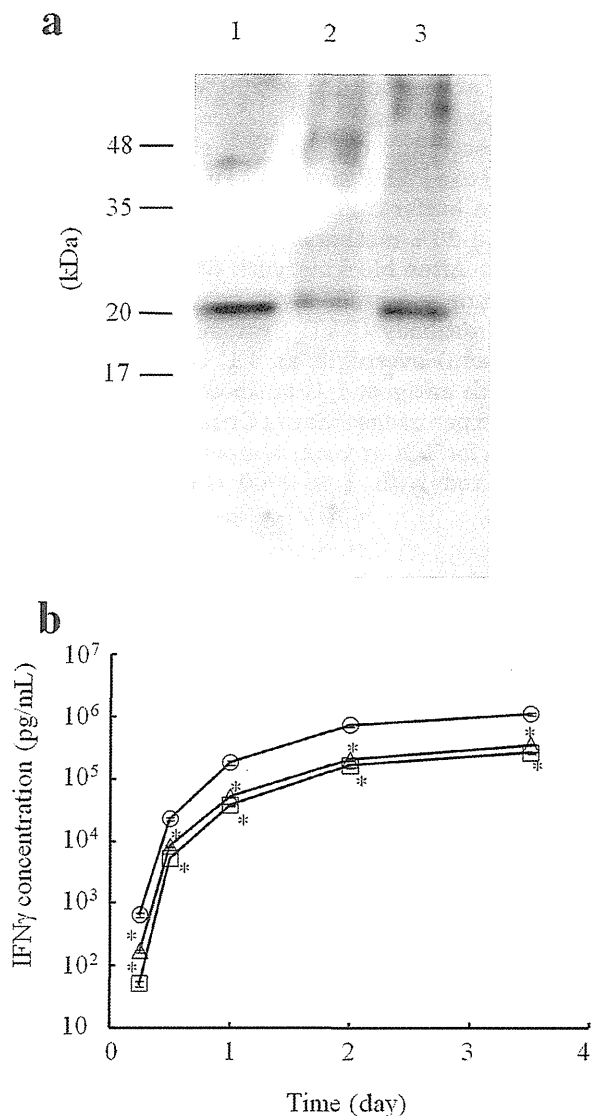


**Figure 1.** Expression of IFN $\gamma$ -ABP and ABP-IFN $\gamma$  in COS-7 cells. (a) Western blot analysis of IFN $\gamma$ , IFN $\gamma$ -ABP, and ABP-IFN $\gamma$ . Western blotting was performed to confirm the molecular weight of IFN $\gamma$  (lane 1), ABP-IFN $\gamma$  (lane 2), and IFN $\gamma$ -ABP (lane 3). Culture media of COS-7 cells transfected with pCMV-IFN $\gamma$ , pCMV-ABP-IFN $\gamma$ , and pCMV-IFN $\gamma$ -ABP were subjected to 12.5% SDS-PAGE under reducing conditions. IFN $\gamma$ , ABP-IFN $\gamma$ , and IFN $\gamma$ -ABP were detected with antimouse IFN $\gamma$  polyclonal antibody. (b) Time course of the concentration of IFN $\gamma$  (circles), IFN $\gamma$ -ABP (squares), and ABP-IFN $\gamma$  (triangles) in the culture medium of COS-7 cells after transfection of pCMV-IFN $\gamma$ , pCMV-IFN $\gamma$ -ABP, and pCMV-ABP-IFN $\gamma$  (2  $\mu$ g/mL). At the indicated time periods after transfection, the supernatants were collected and the concentration of IFN $\gamma$ , ABP-IFN $\gamma$ , or IFN $\gamma$ -ABP was measured by ELISA using antimouse IFN $\gamma$  antibody. The results are expressed as the mean  $\pm$  standard error of the mean (SEM) of three independent determinations. \* $p < 0.05$  compared with pCMV-IFN $\gamma$  group.

COS-7 cells. Under reducing conditions, a band around 20 kDa was detected in the culture media of cells transfected with pCMV-IFN $\gamma$  (lane 1), which is in good agreement with the size of monomeric IFN $\gamma$ .<sup>23</sup> The supernatant of cells transfected with pCMV-IFN $\gamma$ -ABP or pCMV-ABP-IFN $\gamma$  also showed a band of slightly higher molecular mass of IFN $\gamma$  (lanes 2 and 3, respectively), suggesting that the fusion proteins, IFN $\gamma$ -ABP and ABP-IFN $\gamma$ , were expressed from the plasmid vectors.

Figure 1b shows the time course of IFN $\gamma$ , IFN $\gamma$ -ABP, and ABP-IFN $\gamma$  concentrations in culture media of COS-7 cells after transfection with pCMV-IFN $\gamma$ , pCMV-IFN $\gamma$ -ABP, or pCMV-ABP-IFN $\gamma$ , respectively. The concentrations of IFN $\gamma$ -ABP and ABP-IFN $\gamma$  were significantly lower than that of IFN $\gamma$ , although the shapes of the time courses were similar among all the groups.

#### Measurement of the Biological Activity of IFN $\gamma$ -ABP and ABP-IFN $\gamma$

The biological activity of IFN $\gamma$ -ABP and ABP-IFN $\gamma$  was measured by GAS-dependent luciferase assay (Fig. 2a).<sup>11,24,25</sup> Addition of IFN $\gamma$  to cells transfected with pGAS-Luc increased the luciferase activity of the cells in a concentration-dependent manner, confirming the validity of the method. IFN $\gamma$ -ABP or ABP-IFN $\gamma$  also dose-dependently increased the luciferase activity. The calculated EC<sub>50</sub> values of IFN $\gamma$ -ABP and ABP-IFN $\gamma$  were 93 and 110 pg/mL, respectively, which indicates that IFN $\gamma$ -ABP and ABP-IFN $\gamma$  possess 46% and 40% of the activity of IFN $\gamma$  (43 pg/mL). Thus, high biological activity remained after the fusion of ABP to IFN $\gamma$  irrespective of the fusion sites. There was no significant difference in activity between IFN $\gamma$ -ABP and ABP-IFN $\gamma$ .

To investigate whether the biological activity of IFN $\gamma$ , IFN $\gamma$ -ABP, and ABP-IFN $\gamma$  is affected by MSA, the GAS-dependent assay was carried out using IFN $\gamma$ , IFN $\gamma$ -ABP, or ABP-IFN $\gamma$  incubated with or without 0.25 mg/mL of MSA (Fig. 2b). Presence of MSA hardly affected the activity of IFN $\gamma$ , but it significantly reduced that of IFN $\gamma$ -ABP and ABP-IFN $\gamma$ .

#### Binding Affinity of IFN $\gamma$ -ABP and ABP-IFN $\gamma$ to Albumin

Figure 3 shows the amount of IFN $\gamma$ , IFN $\gamma$ -ABP, and ABP-IFN $\gamma$  bound to MSA immobilized onto culture plates, determined using ELISA with anti-mouse IFN $\gamma$  antibody. Both IFN $\gamma$ -ABP and ABP-IFN $\gamma$  bound to MSA in a dose-dependent manner. On the contrary, IFN $\gamma$  hardly bound to MSA. The amount of ABP-IFN $\gamma$  bound to MSA was significantly higher than that of IFN $\gamma$ -ABP compared at the same concentrations, indicating the high affinity of the former. The fusion proteins showed much less binding to human serum albumin or bovine IgG (data not shown).

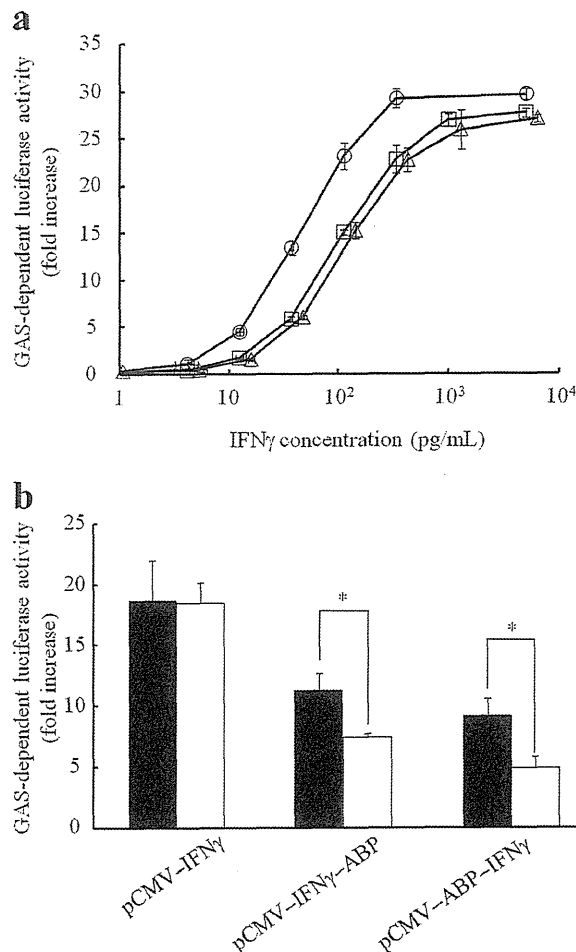


**Figure 2.** (a) Biological activity of IFN $\gamma$ -ABP and ABP-IFN $\gamma$ . B16-BL6 cells transfected with pGAS-Luc and phRL-TK were incubated with serial dilutions of IFN $\gamma$  (circles), IFN $\gamma$ -ABP (squares), or ABP-IFN $\gamma$  (triangles) for a further 24 h. pGAS-Luc, plasmid DNA expressing firefly luciferase, was used to assess the degree of activation of the GAS signaling pathway. phRL-TK, plasmid DNA expressing renilla luciferase was used for normalization of the transfection efficiency and cell numbers. The ratio was normalized to give  $x$ -fold values relative to those of the untreated group and the half-maximum effective concentration (EC<sub>50</sub>) of IFN $\gamma$ , IFN $\gamma$ -ABP, and ABP-IFN $\gamma$  was calculated. The results are expressed as the mean  $\pm$  SEM of four independent determinations. (b) Biological activity of IFN $\gamma$ , IFN $\gamma$ -ABP, and ABP-IFN $\gamma$  with or without MSA. IFN $\gamma$ , IFN $\gamma$ -ABP, and ABP-IFN $\gamma$  (100 pg/mL) incubated with (open column) or without (closed column) 0.25 mg/mL MSA was added to B16-BL6 cells transfected with pGAS-Luc and phRL-TK. The results are expressed as the mean  $\pm$  SEM of four independent determinations. \* $p < 0.05$ .

#### Clearance of IFN $\gamma$ , IFN $\gamma$ -ABP, and ABP-IFN $\gamma$ after Intravenous Injection into Mice

To confirm whether the fusion of ABP increases the blood circulation time of IFN $\gamma$ , IFN $\gamma$ -ABP, and

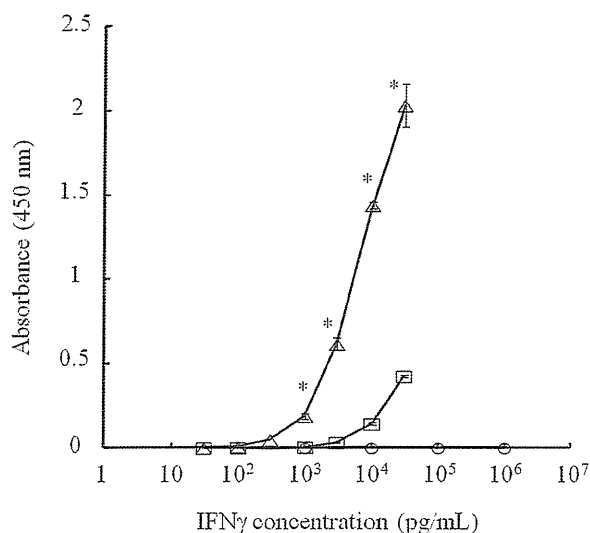


**Figure 3.** Binding of IFN $\gamma$ -ABP and ABP-IFN $\gamma$  to immobilized MSA. MSA was immobilized onto 96-well plates at a concentration of 2  $\mu$ g/mL overnight. IFN $\gamma$  (circles), IFN $\gamma$ -ABP (squares), or ABP-IFN $\gamma$  (triangles) was serially diluted and 100  $\mu$ L amounts were added per well. After incubation for 2 h, bound proteins were detected by ELISA using antimouse IFN $\gamma$  antibody. The results are expressed as the mean  $\pm$  SEM of three independent determinations. \* $p < 0.05$  compared with IFN $\gamma$ -ABP group at the same concentration.

**Table 1.** Pharmacokinetic Parameters of IFN $\gamma$ , IFN $\gamma$ -ABP, and ABP-IFN $\gamma$  after Intravenous Injection into Mice

Protein	IFN $\gamma$	IFN $\gamma$ -ABP	ABP-IFN $\gamma$
AUC (ng h/mL)	57.6 $\pm$ 2.6	270 $\pm$ 24*	458 $\pm$ 5*
MRT (h)	2.64 $\pm$ 0.14	2.64 $\pm$ 0.07	4.11 $\pm$ 0.20*

The AUC and MRT were calculated by integration to infinite time, and the mean  $\pm$  SEM values are shown.

\*Statistically significant ( $p < 0.05$ ) compared with IFN $\gamma$ .

ABP-IFN $\gamma$  were injected into the tail vein of mice. Figure 4 shows the time courses of the concentrations of IFN $\gamma$ , IFN $\gamma$ -ABP, and ABP-IFN $\gamma$  in the serum after intravenous injection into mice at a dose of 8.5  $\mu$ g IFN $\gamma$ /kg body weight. The clearance of IFN $\gamma$ -ABP and ABP-IFN $\gamma$  was slower than that of IFN $\gamma$ . The profiles were evaluated by moment analysis to calculate the AUC and MRT (Table 1). The AUC of IFN $\gamma$ -ABP (270 ng h/mL) and ABP-IFN $\gamma$  (458 ng h/mL) was significantly greater than that of IFN $\gamma$  (57.6 ng h/mL). In addition, the MRT of ABP-IFN $\gamma$  (4.11 h) was significantly longer than that of IFN $\gamma$  (2.64 h) or IFN $\gamma$ -ABP (2.69 h).

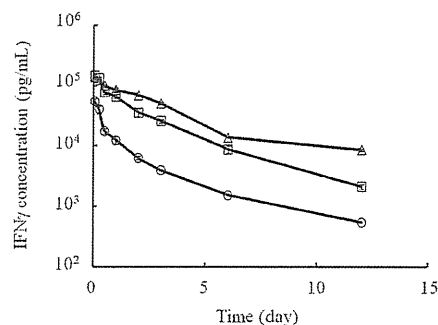


**Figure 4.** Clearance of IFN $\gamma$ , IFN $\gamma$ -ABP, and ABP-IFN $\gamma$  after intravenous injection into mice. The concentrations of IFN $\gamma$  (circles), IFN $\gamma$ -ABP (squares), and ABP-IFN $\gamma$  (triangles) were measured by ELISA using antimouse IFN $\gamma$  antibody. The results are expressed as the mean  $\pm$  SEM of four mice.

#### mRNA Expression of IFN $\gamma$ , IFN $\gamma$ -ABP, and ABP-IFN $\gamma$ in the Liver and Time Course of the Serum Concentration of IFN $\gamma$ , IFN $\gamma$ -ABP, and ABP-IFN $\gamma$ after In Vivo Gene Transfer

Figure 5a shows the mRNA expression of IFN $\gamma$ , IFN $\gamma$ -ABP, and ABP-IFN $\gamma$  in the liver at 6 h after hydrodynamic injection of pCMV-IFN $\gamma$ , pCMV-IFN $\gamma$ -ABP, or pCMV-ABP-IFN $\gamma$ , respectively. The expression of IFN $\gamma$ , IFN $\gamma$ -ABP, and ABP-IFN $\gamma$  was not significantly different from one another. Figure 5b shows the time courses of the serum concentrations of IFN $\gamma$ , IFN $\gamma$ -ABP, and ABP-IFN $\gamma$  after hydrodynamic injection of pCMV-IFN $\gamma$ , pCMV-IFN $\gamma$ -ABP, or pCMV-ABP-IFN $\gamma$ , respectively, at a dose of 0.2 pmol/mouse. The disappearance of IFN $\gamma$ -ABP and ABP-IFN $\gamma$  from the circulation was much slower than that of IFN $\gamma$ . The  $C_{max}$  of IFN $\gamma$ -ABP (516 ng/mL) and ABP-IFN $\gamma$  (1940 ng/mL) was markedly greater than that of IFN $\gamma$  (46.6 ng/mL). The time to reach the maximum serum concentration ( $t_{max}$ ) of the fusion proteins was 0.5 (IFN $\gamma$ -ABP) and 1 (ABP-IFN $\gamma$ ) day, which was later than that of IFN $\gamma$  (0.25 day). Table 2 summarizes the AUC and MRT values after hydrodynamic injection of pCMV-IFN $\gamma$ , pCMV-IFN $\gamma$ -ABP, and pCMV-ABP-IFN $\gamma$ . A hydrodynamic injection of pCMV-IFN $\gamma$ -ABP or pCMV-ABP-IFN $\gamma$  produced about a 25- or 140-fold greater AUC and a 1.5- or twofold longer MRT than seen with pCMV-IFN $\gamma$ .

#### Inhibition of the Growth of Metastatic Pulmonary Tumor by Gene Transfer of IFN $\gamma$ , IFN $\gamma$ -ABP, or ABP-IFN $\gamma$ in Mice

Figure 6 shows the number of metastatic colonies of CT-26 cells on the lung surface at 14 days after inoculation of CT-26 cells into the tail vein of mice. A hydrodynamic injection of pCMV-IFN $\gamma$ , pCMV-IFN $\gamma$ -ABP, or pCMV-ABP-IFN $\gamma$  signifi-

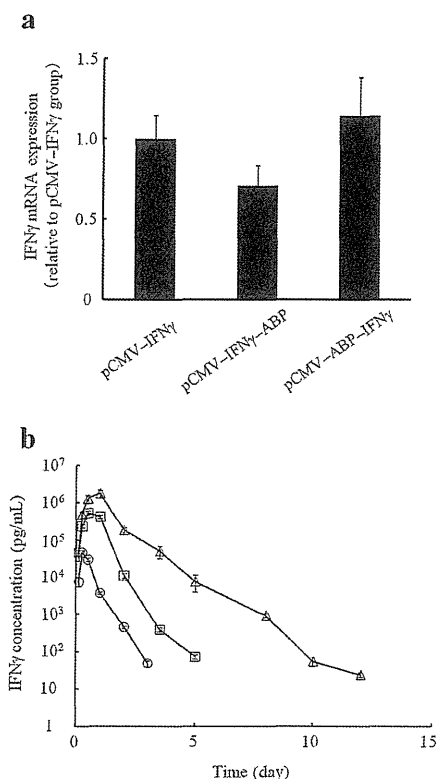


**Figure 5.** (a) mRNA expression of IFN $\gamma$ , IFN $\gamma$ -ABP, and ABP-IFN $\gamma$  in the liver. mRNA expression of IFN $\gamma$ , IFN $\gamma$ -ABP, and ABP-IFN $\gamma$  in the liver was measured 6 h after hydrodynamic injection of pCMV-IFN $\gamma$ , pCMV-IFN $\gamma$ -ABP, or pCMV-ABP-IFN $\gamma$  into mice. The results are expressed as the mean  $\pm$  SEM of three mice. (b) Time courses of the concentrations of IFN $\gamma$ , IFN $\gamma$ -ABP, and ABP-IFN $\gamma$  in the serum after hydrodynamic injection of pCMV-IFN $\gamma$ , pCMV-IFN $\gamma$ -ABP, or pCMV-ABP-IFN $\gamma$  into mice. Each plasmid DNA was administered at a dose of 0.2 pmol/mouse. The concentrations of IFN $\gamma$  (circles), IFN $\gamma$ -ABP (squares), and ABP-IFN $\gamma$  (triangles) were measured by ELISA using antimouse IFN $\gamma$  antibody. The results are expressed as the mean  $\pm$  SEM of three mice.

**Table 2.** Pharmacokinetic Parameters of IFN $\gamma$ , IFN $\gamma$ -ABP, and ABP-IFN $\gamma$  after Hydrodynamic Injection of pCMV-IFN $\gamma$ , pCMV-IFN $\gamma$ -ABP, and pCMV-ABP-IFN $\gamma$ , Respectively, into Mice

	IFN $\gamma$	IFN $\gamma$ -ABP	ABP-IFN $\gamma$
AUC (ng h/mL)	24.3 $\pm$ 2.6	569 $\pm$ 58*	3430 $\pm$ 430*
MRT (h)	0.49 $\pm$ 0.01	0.79 $\pm$ 0.01*	1.03 $\pm$ 0.02*
C <sub>max</sub> (ng/mL)	46.6 $\pm$ 3.2	516 $\pm$ 60*	1940 $\pm$ 240*
t <sub>max</sub> (h)	6	12	24

The C<sub>max</sub> and t<sub>max</sub> values were obtained from actual data recorded after hydrodynamic injection of pCMV-IFN $\gamma$ , pCMV-IFN $\gamma$ -ABP, and pCMV-ABP-IFN $\gamma$  at a dose of 0.2 pmol/mouse. The AUC and MRT were calculated by integration to infinite time, and the mean  $\pm$  SEM values are shown.

\*Statistically significant ( $p < 0.05$ ) compared with pCMV-IFN $\gamma$ .

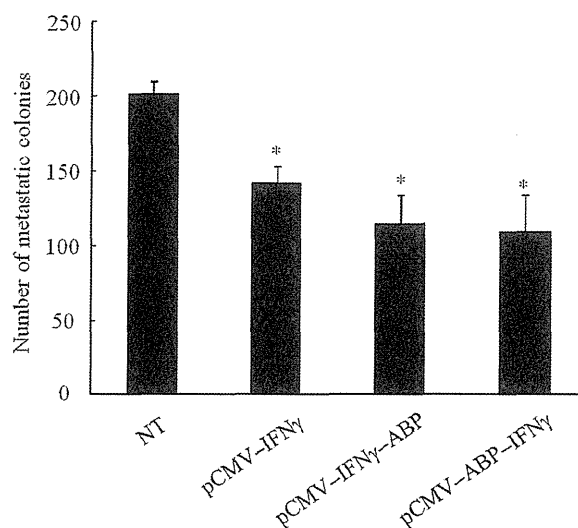


**Figure 6.** Number of metastatic colonies of CT-26 cells on the lung surface of mice. Pulmonary metastasis was induced by inoculation of  $1 \times 10^5$  CT-26 cells into a tail vein (day 0). On day 3, pCMV-IFN $\gamma$ , pCMV-IFN $\gamma$ -ABP, or pCMV-ABP-IFN $\gamma$  was injected into mice by hydrodynamic injection at a dose of 0.7 pmol/mouse. A group of control mice was left untreated (NT). At 14 days after tumor inoculation, mice were sacrificed and the number of metastatic colonies on the lung surface was counted. The results are expressed as the mean  $\pm$  SEM of five mice. \* $p < 0.05$  compared with the NT group.

cantly reduced the number of colonies to 70%, 56%, or 53% that in the no treatment group, respectively. There was no significant difference in the number of metastatic colonies among the groups.

**DISCUSSION**

Our previous study showed that the fusion of MSA to IFN $\gamma$  dramatically improved the pharmacokinetic properties of IFN $\gamma$ . However, the fusion also greatly reduced the biological activity of IFN $\gamma$ .<sup>11</sup> Such reduction in the activity is similar to that of polyethylene glycol-conjugated human IFN $\alpha$  products used in clinical settings.<sup>26</sup> These results suggest that the use of serum albumin or other macromolecules is not suitable for the control of the pharmacokinetics of IFN $\gamma$ . The present study clearly demonstrates that the fusion of a much smaller peptide (20 amino acids) than MSA is useful for controlling the tissue distribution of IFN $\gamma$  without significantly reducing its biological activity.

Both IFN $\gamma$ -ABP and ABP-IFN $\gamma$  exhibited about 50% the activity of IFN $\gamma$ , suggesting that the site of the fusion of ABP is of little importance. In addition, the reduced activity of IFN $\gamma$ -ABP and ABP-IFN $\gamma$

in the presence of MSA (Fig. 2b) strongly suggests that the binding of IFN $\gamma$ -ABP and ABP-IFN $\gamma$  with MSA somewhat interferes with the binding of these fusion proteins to IFN $\gamma$  receptor. It has been reported that both the N- and C-terminals of IFN $\gamma$  are critical for the receptor interaction.<sup>27,28</sup> Because bioactive IFN $\gamma$  is an antiparallel dimer,<sup>1,29</sup> fusion at either end would have a similar impact on the physiochemical properties of IFN $\gamma$ . On the contrary, ABP-IFN $\gamma$  exhibited higher binding affinity to MSA than IFN $\gamma$ -ABP (Fig. 3), indicating that the fusion site did affect the interaction with MSA. A crystal structure analysis of human IFN $\gamma$  revealed that both the N- and C-terminals are located on the surface of the molecule and the N-terminal is more flexible than the C-terminal which has some adjacent side chains.<sup>30,31</sup> Although there is little information on the structural properties of mouse IFN $\gamma$ , the helix of IFN $\gamma$  is strongly conserved between mice and humans.<sup>30,32</sup> Therefore, the stronger binding activity of ABP-IFN $\gamma$  to MSA, compared with IFN $\gamma$ -ABP, is probably due to the greater flexibility of the N-terminal domain compared with the C-terminal.

Reflecting the binding to MSA, the fusion of ABP could prolong the circulation time of IFN $\gamma$ . Similar results were observed after gene delivery of these derivatives. An injection of pCMV-ABP-IFN $\gamma$  produced a higher AUC and longer MRT than that of pCMV-IFN $\gamma$ -ABP (Table 2). These differences would be due to the difference in the binding affinity to MSA between these fusion proteins, as was the case with the protein injection, because the mRNA expression of IFN $\gamma$  in the liver was comparable among all the groups (Fig. 5a). Taken together, these results clearly show that the gene delivery of IFN $\gamma$ -ABP or ABP-IFN $\gamma$  is an effective approach to improving the pharmacokinetic properties of IFN $\gamma$ .

Effective inhibition of metastatic tumor growth by gene delivery of IFN $\gamma$ -ABP or ABP-IFN $\gamma$  indicates that these fusion proteins are pharmacologically active and their gene delivery is a promising therapeutic method for the treatment of a number of diseases. Although the affinity of IFN $\gamma$ -ABP for MSA was higher than that of ABP-IFN $\gamma$ , and no significant difference was observed in the number of metastatic colonies. A possible explanation of this is that the high affinity of the fusion protein for MSA disturbs its binding to the IFN $\gamma$  receptor, as observed in the *in vitro* experiment (Fig. 2b). The results of the present study indicate that selecting or designing ABP with proper affinity for serum albumin can maximize the therapeutic effects of IFN $\gamma$  by achieving optimal balance between biological activity and retention in blood circulation.

## CONCLUSION

We have demonstrated that the fusion of ABP to IFN $\gamma$  is a useful approach to achieving prolonged retention

in blood circulation through binding to serum albumin and this prolonged retention is effective in inhibiting metastatic tumor growth in mouse lung.

## ACKNOWLEDGMENTS

This work was supported in part by a Grant-in-Aid for Scientific Research (B) from the Japan Society for the Promotion of Science, and by a Grant-in-Aid for Research on Hepatitis from the ministry of Health, Labour, and Welfare of Japan.

## REFERENCES

- Farrar MA, Schreiber RD. 1993. The molecular cell biology of interferon- $\gamma$  and its receptor. *Annu Rev Immunol* 11:571-611.
- Jonasch E, Haluska FG. 2001. Interferon in oncological practice: Review of interferon biology, clinical applications, and toxicities. *Oncologist* 6:34-55.
- Younes HM, Amsdem BG. 2002. Interferon- $\gamma$  therapy: Evaluation of routes of administration and delivery systems. *J Pharm Sci* 91:2-17.
- Miller CH, Maher SG, Young HA. 2009. Clinical use of interferon- $\gamma$ . *Ann N Y Acad Sci* 1182:69-79.
- Kurzrock R, Rosenblum MG, Sherwin SA, Rios A, Talpaz M, Quesada JR, Gutterman JU. 1985. Pharmacokinetics, single-dose tolerance, and biological activity of recombinant gamma-interferon in cancer patients. *Cancer Res* 45:2866-2872.
- Ferenci P, Brunner H, Nachbaur K, Datz C, Gschwantler M, Hofer H, Stauber R, Hackl F, Jessner W, Rosenbeiger M, Steindl PM, Hegenbarth K, Gangl A, Vogel W. 2001. Combination of interferon induction therapy and ribavirin in chronic hepatitis C. *Hepatology* 34:1006-1011.
- Kobayashi N, Kuramoto T, Chen S, Watanabe Y, Takakura Y. 2002. Therapeutic effect of intravenous interferon gene delivery with naked plasmid DNA in murine metastasis model. *Mol Ther* 6:737-744.
- Kawano H, Nishikawa M, Mitsui M, Takahashi Y, Kako K, Yamaoka K, Watanabe Y, Takakura Y. 2007. Improved anti-cancer effect of interferon gene transfer by sustained expression using CpG-reduced plasmid DNA. *Int J Cancer* 121:401-406.
- Hattori K, Nishikawa M, Watcharanurak K, Ikoma A, Kabashima K, Toyota H, Takahashi Y, Takahashi R, Watanabe Y, Takakura Y. 2010. Sustained exogenous expression of therapeutic levels of IFN- $\gamma$  ameliorates atopic dermatitis in NC/Nga mice via Th1 polarization. *J Immunol* 184:2729-2735.
- Watcharanurak K, Nishikawa M, Takahashi Y, Kabashima K, Takahashi R, Takakura Y. 2013. Regulation of immunological balance by sustained interferon- $\gamma$  gene transfer for acute phase of atopic dermatitis in mice. *Gene Ther* [Epub ahead of print.]
- Miyakawa N, Nishikawa M, Takahashi Y, Ando M, Misaka M, Watanabe Y, Takakura Y. 2011. Prolonged circulation half-life of interferon  $\gamma$  activity by gene delivery of interferon  $\gamma$ -serum albumin fusion protein in mice. *J Pharm Sci* 100:2350-2357.
- Subramanian GM, Fiscella M, Smith AL, Zeuzem S, McHutchison JG. 2007. Albinterferon  $\alpha$ -2b: a genetic fusion protein for the treatment of chronic hepatitis C. *Nat Biotechnol* 25:1411-1419.
- Dennis MS, Zhang M, Meng YG, Kadkhodayan M, Kirchofer D, Combs D, Damico LA. 2002. Albumin binding as a general strategy for improving the pharmacokinetics of proteins. *J Biol Chem* 277:35035-35043.

14. Nguyen A, Reyes AE II, Zhang M, McDonald P, Wong WL, Damico LA, Dennis MS. 2005. The pharmacokinetics of an albumin-binding Fab (AB.Fab) can be modulated as a function of affinity for albumin. *Protein Eng Des Sel* 19:291–297.
15. Dennis MS, Jin H, Dugger D, Yang R, McFarland L, Ogasawara A, Williams C, Cole MJ, Ross S, Schwall R. 2005. Imaging tumors with an albumin-binding Fab, a novel tumor-targeting agent. *Clin Cancer Res* 11:7109–7121.
16. Kanno Y, Kozak CA, Schindler C, Driggers PH, Ennist DL, Gleason SL, Darnell JE Jr, Ozato K. 1993. The genomic structure of the murine ICSBP gene reveals the presence of the gamma interferon-responsive element, to which an ISGF3  $\alpha$  subunit (or similar) molecule binds. *Mol Cell Biol* 13:3951–3963.
17. Zhao HL, Yao XQ, Xue C, Wang Y, Xiong XH, Liu ZM. 2008. Increasing the homogeneity, stability and activity of human serum albumin and interferon- $\alpha$ 2b fusion protein by linker engineering. *Protein Expr Purif* 61:73–77.
18. Takahashi Y, Kaneda H, Takasuka N, Hattori K, Nishikawa M, Takakura Y. 2008. Enhancement of antiproliferative activity of interferons by RNA interference-mediated silencing of SOCS gene expression in tumor cells. *Cancer Sci* 99:1650–1655.
19. Liu F, Song YK, Liu D. 1999. Hydrodynamics-based transfection in animals by systemic administration of plasmid DNA. *Gene Ther* 6:1258–1266.
20. Zhang GF, Budker V, Wolff JA. 1999. High levels of foreign gene expression in hepatocytes after tail vein injections of naked plasmid DNA. *Hum Gene Ther* 10:1735–1737.
21. Mitsui M, Nishikawa M, Zang L, Ando M, Hattori K, Takahashi Y, Watanabe Y, Takakura Y. 2009. Effect of the content of unmethylated CpG dinucleotides in plasmid DNA on the sustainability of transgene expression. *J Gene Med* 11:435–443.
22. Yamaoka K, Nakagawa T, Uno T. 1978. Statistical moments in pharmacokinetics. *J Pharmacokinet Biopharm* 6:547–558.
23. Gribaudo G, Cofano F, Prat M, Baiocchi C, Cavallo G, Landolfo S. 1985. Natural murine interferon- $\gamma$ . *J Biol Chem* 260:9936–9940.
24. Schroder K, Hertzog PJ, Ravasi T, Hume DA. 2004. Interferon- $\gamma$ : An overview of signals, mechanisms and functions. *J Leukoc Biol* 75:163–189.
25. Stark GR, Kerr IM, Williams BR, Silverman RH, Schreiber RD. 1998. How cells respond to interferons. *Annu Rev Biochem* 67:227–264.
26. Veronese FM, Pasut G. 2005. PEGylation, successful approach to drug delivery. *Drug Discov Today* 10:1451–1458.
27. Griggs ND, Jarpe MA, Pace JL, Russell SW, Johnson HM. 1992. The N-terminus and C-terminus of IFN- $\gamma$  are binding domains for cloned soluble IFN- $\gamma$  receptor. *J Immunol* 149:517–520.
28. Lundell DJ, Narula SK. 1994. Structural elements required for receptor recognition of human interferon- $\gamma$ . *Pharmacol Ther* 64:1–21.
29. Fountoulakis M, Juranville JF, Maris A, Ozmen L, Garotta G. One interferon  $\gamma$  receptor binds one interferon  $\gamma$  dimer. 1990. *J Biol Chem* 265:169–179.
30. Ealick SE, Cook WJ, Vijay-Kumar S, Carson M, Nagabhushan TL, Trotta PP, Bugg CE. 1991. Three-dimensional structure of recombinant human interferon- $\gamma$ . *Science* 252:698–702.
31. Walter MR, Windsor WT, Nagabhushan TL, Lundell DJ, Lunn CA, Zauodny PJ, Narula SK. 2002. Crystal structure of a complex between interferon- $\gamma$  and its soluble high-affinity receptor. *Nature* 376:230–235.
32. Savan R, Ravichandran S, Collins JR, Sakai M, Young HA. 2009. Structural conservation of interferon  $\gamma$  among vertebrates. *Cytokine Growth Factor Rev* 20:115–124.



Original Article

# Serum RANTES level influences the response to pegylated interferon and ribavirin therapy in chronic hepatitis C

Kazuki Komase,<sup>1</sup> Shinya Maekawa,<sup>1,2</sup> Mika Miura,<sup>1</sup> Ryota Sueki,<sup>1</sup> Makoto Kadokura,<sup>1</sup> Hiroko Shindo,<sup>1</sup> Kuniaki Shindo,<sup>1</sup> Fumitake Amemiya,<sup>1</sup> Yasuhiro Nakayama,<sup>1</sup> Taisuke Inoue,<sup>1,2</sup> Minoru Sakamoto,<sup>1</sup> Atsuya Yamashita,<sup>3</sup> Kohji Moriishi<sup>3</sup> and Nobuyuki Enomoto<sup>1</sup>

<sup>1</sup>First Department of Medicine, Faculty of Medicine, <sup>2</sup>Department of Advanced Medicine for Liver Diseases, Faculty of Medicine, and <sup>3</sup>Department of Microbiology, University of Yamanashi, Yamanashi, Japan

**Aim:** Prediction of treatment responses to pegylated interferon (PEG IFN) plus ribavirin (RBV) therapy is uncertain for genotype 1b chronic hepatitis C.

**Methods:** In this study, 96 patients were investigated for the correlation between 36 pretreatment serum chemokine/cytokine levels and PEG IFN/RBV treatment efficacy by a sandwich enzyme-linked immunoassay (ELISA) and a bead array.

**Results:** First, chemokines/cytokines were measured semi-quantitatively by sandwich ELISA in 31 randomly-selected patients and the serum regulated on activation normal T-cell expressed and secreted (RANTES) level was found to be significantly higher in the sustained virological response (SVR) group than the non-SVR group ( $P = 0.048$ ). Precise RANTES

measurement in all 96 patients using a bead array confirmed this correlation ( $P = 0.002$ ). However, the genetic RANTES haplotype was not significantly related to the serum level. The serum RANTES level was extracted by multivariate analysis (odds ratio = 4.09, 95% confidence interval = 1.02–16.5,  $P = 0.048$ ) as an independent variable contributing to SVR.

**Conclusion:** The serum RANTES level is an important determinant influencing the virological response to PEG IFN/RBV therapy in chronic hepatitis C.

**Key words:** hepatitis C virus, pegylated interferon plus ribavirin therapy, RANTES

## INTRODUCTION

HEPATITIS C VIRUS (HCV) is a major cause of chronic liver disease worldwide and persistent infection may lead to liver cirrhosis and hepatocellular carcinoma.<sup>1</sup> Therapy leading to HCV eradication is the only treatment with proven efficacy in decreasing the occurrence of hepatocellular carcinoma.<sup>2</sup> Recently, treatment with telaprevir, a non-structural (NS)3/4A protease inhibitor, combined with pegylated interferon

(PEG IFN) and ribavirin (RBV), increased the rates of sustained viral response (SVR) up to 64–75%<sup>3,4</sup> compared to the SVR rate of approximately 50% for the previous PEG IFN/RBV therapy. However, it has become evident that genotype 1-infected patients with a null response to previous PEG IFN/RBV therapy have poor responses to PEG IFN/RBV/telaprevir,<sup>5</sup> with an SVR rate as low as approximately 30%, illustrating the difficulty in treating patients infected with genotype 1 HCV. Therefore, precise and accurate prediction of the viral response to PEG IFN/RBV therapy remains an important issue.

Treatment resistance is attributed to various factors associated with the virus and host. Viral factors, such as amino acid (a.a.) sequence variation in the core and NS5A regions, have been investigated extensively for their contribution to the outcome of IFN-based therapy,<sup>6,7</sup> including PEG IFN/RBV therapy. On the other hand, host factors such as African-American race, older age, being obese, the presence of cirrhosis and

Correspondence: Dr Shinya Maekawa, First Department of Medicine, Faculty of Medicine, University of Yamanashi, 1110 Shimokato, Chuo, Yamanashi 409-3898, Japan. Email: maekawa@yamanashi.ac.jp

Conflict of interest: Shinya Maekawa and Taisuke Inoue belong to a donation-funded department that is funded by MSD (Tokyo, Japan). Nobuyuki Enomoto received research funding from MSD (Tokyo, Japan) and Roche (Tokyo, Japan).

Received 26 September 2012; revision 18 November 2012; accepted 26 November 2012.

steatosis, and insulin resistance have been reported to be associated with treatment resistance.<sup>8–11</sup> Especially, single nucleotide polymorphisms (SNP) near the interleukin (*IL*)-28B gene, including rs12979860 and rs8099917, have been reported to have a significant correlation with the response to IFN-based therapy.<sup>12,13</sup> However, even with inclusion of these factors, prediction of the treatment response in chronic HCV infection remains uncertain at present.

Chemokines are a group of small, exogenously secreted cytokines that modulate the migration of leukocytes to sites of tissue damage and inflammation in a variety of infectious and autoimmune diseases.<sup>14</sup> In chronic HCV infection, chemokines such as *RANTES* (regulated on activation normal T-cell expressed and secreted), macrophage inflammatory protein (*MIP*)-1 $\alpha$ , *MIP*-1 $\beta$  and interferon- $\gamma$  inducible protein 10 kDa (*IP*-10) are elevated and considered to play crucial roles in inflammatory processes and viral elimination, as well as the transition from innate to adaptive immunity.<sup>14,15</sup> Upregulation of several serum chemokines, such as eotaxin, *IP*-10 and *RANTES* also has been reported in HCV infection, possibly reflecting hepatic inflammation.<sup>16</sup> Considering the roles of chemokines/cytokines in establishing chronic hepatitis, it is possible that these chemokines also affect the response to antiviral therapy, and actually several chemokines as interleukin (*IL*)-8, *IL*-10, *MIP*-1 $\beta$ , *RANTES* or *IP*-10 have been investigated previously for their association with the treatment response.<sup>16–20</sup> However, the importance of those chemokines has not been established yet and, moreover, these studies did not characterize in detail these chemokines in association with other factors, including *IL*-28B influencing the response to therapy.

In this study, we explored extensively the association of 36 serum cytokines/chemokines and the treatment response, with detailed information of host and virus, to predict better the treatment response to PEG IFN and RBV therapy in genotype 1b HCV infection. Because the pretreatment serum *RANTES* level was found to be correlated significantly with the response, we analyzed further the association between the serum level of *RANTES* and the genomic SNP.

## METHODS

### Patients

NINETY-SIX CONSECUTIVE PATIENTS with genotype 1b HCV and receiving PEG IFN/RBV therapy between 2004 and 2010 at Yamanashi University Hospital were recruited retrospectively into the study. All

patients received the standard therapy according to the treatment protocol of PEG IFN/RBV therapy for Japanese patients, established by a hepatitis study group of the Ministry of Health, Labor and Welfare, Japan (PEG IFN- $\alpha$ -2b 1.5  $\mu$ g/kg bodyweight, once weekly s.c., and RBV 600–800 mg daily p.o. for 48 weeks).<sup>21</sup> All patients enrolled fulfilled the following criteria: (i) negative for hepatitis B surface antigen; (ii) no other forms of hepatitis, such as primary biliary cirrhosis, autoimmune liver disease or alcoholic liver disease; (iii) not co-infected with HIV; and (iv) a signed consent was obtained for the study protocol that had been approved by the Human Ethics Review Committee of Yamanashi University Hospital. The study was approved by the ethics committees of University of Yamanashi, and the study protocol conformed to the ethical guidelines of the 2008 Declaration of Helsinki.

### Definition of treatment outcome

An SVR was defined as undetectable serum HCV RNA at 24 weeks after the end of treatment. Relapse was defined as reappearance of detectable HCV RNA levels following discontinuation of treatment. Null response was defined as less than 2 log decrease of the baseline HCV RNA levels after 12 weeks of treatment. Based on this definition, when patients were classified according to the achievement of SVR, patients with relapse or null response were classified as non-SVR.

### Serum cytokine measurement

#### Sandwich enzyme-linked immunosorbent assay (ELISA)

Blood samples were collected before initiation of treatment and were stored at  $-80^{\circ}\text{C}$  until use. Semiquantitation of serum cytokines was performed using the Proteome Profiler Human Cytokine Array Kit Panel A (R&D Systems, Minneapolis, CA, USA) according to the manufacturer's instructions. The kit consists of a nitrocellulose membrane containing 36 different anti-cytokine antibodies (anti-C5a, anti-CD154, anti-G-CSF, anti-GM-CSF, anti-CXCL1, anti-CCL1, anti-sICAM-1, anti-IFN- $\gamma$ , anti-IL-1 $\alpha$ , anti-IL-1 $\beta$ , anti-IL-1ra, anti-IL-2, anti-IL-4, anti-IL-5, anti-IL-6, anti-IL-8, anti-IL-10, anti-IL-12p70, anti-IL-13, anti-IL-16, anti-IL-17, anti-IL-17E, anti-IL-23, anti-IL-27, anti-IL-32 $\alpha$ , anti-IP-10, anti-CXCL11, anti-CCL2, anti-MIF, anti-CCL3, anti-CCL4, anti-PAI-1, anti-RANTES, anti-CXCL12, anti-TNF- $\alpha$ , anti-sTREM-1), spotted in duplicate. Serum samples were diluted and mixed with a cocktail of biotinylated detection antibodies. The sample/antibody mixture

was then incubated with the membrane. Any cytokine/detection antibody complex present was bound to the membrane by its cognate immobilized capture antibody. Following washing to remove unbound material, streptavidin-horseradish peroxidase and chemiluminescent detection reagents (ECL Western Blotting Analysis System; GE Healthcare, Buckinghamshire, UK) were added sequentially. Arrays were scanned using a LAS-3000 mini-luminescent image analyzer (Fujifilm, Tokyo, Japan) and were quantified for the densities using Multi Gauge ver. 3.0 software (Fujifilm). Concentrations of cytokines and chemokines were expressed as their signal intensity ratios relative to that of the positive control spotted on the same membrane.

#### Bead array

Precise serum concentrations of regulated on *RANTES* were measured using the Luminex Bio-Plex system (Bio-Rad, Hercules, CA, USA) and the Procarta Cytokine Assay Kit (Panomics, Fremont, CA, USA) in a 96-well plate ELISA-based format according to the manufacturers' recommendations. The sensitivity of the assays is greater than 10 pg/mL cytokine. Serum and standards were incubated with a mixture of the Luminex antibody-conjugated beads for 30 min with constant shaking. After washing, the detection antibodies and substrates were added and incubated for another 30 min. Fluorescent signals were collected and data expressed, using internal standards, in pg/mL as the mean of two individual experiments carried out in duplicate.

#### Viral core and interferon sensitivity-determining region (ISDR) sequence determination by direct sequencing

Hepatitis C virus RNA extraction from serum samples, complementary DNA synthesis and amplification by two-step nested polymerase chain reaction (PCR) were carried out using specific primers for the HCV core and ISDR. PCR amplicons were sequenced directly by Big Dye Terminator ver. 3.1 (ABI, Tokyo, Japan) with universal M13 forward and reverse primers using an ABI prism 3130 sequencer (ABI). The sequence files generated were assembled using Vector NTI software (Invitrogen, Tokyo, Japan) and base-calling errors were corrected following inspection of the chromatogram.

#### SNP typing of the *RANTES* and *IL-28B* genes

Genomic DNA of the patients was extracted from peripheral blood using a blood DNA extraction kit

(QIAGEN, Tokyo, Japan) according to the manufacturer's protocol. The allele typing of each DNA sample was performed by real-time PCR with a model 7500 (ABI) using FAM-labeled SNP primers for the loci rs2107538, rs2280788, rs2280789, rs4796120 and rs3817655 (ABI) for *RANTES* and the locus rs8099917 (ABI) for *IL-28B*.

#### Statistical analysis

Student's *t*-test and Mann-Whitney *U*-test were used to analyze continuous variables, as appropriate. Fisher's exact test was used for the analysis of categorical variables. Receiver-operator curve (ROC) analyses were performed to establish cut-off values for serum cytokine concentration. The optimum cut-off was defined as the value that maximized the area under the ROC. Spearman's correlation coefficient (*R*) was calculated to clarify the strength of relationship between the pretreatment serum cytokine concentrations and clinical parameters. Variables that achieved statistical significance ( $P < 0.05$ ) in univariate analysis were entered into multiple logistic regression analysis to identify significant independent factors. The odds ratios and 95% confidence intervals also were calculated. Data were analyzed using Ekuseru-Toukei 2008 (SSRL, Tokyo, Japan). The haplotype block among rs2107538, rs2280788, rs2280789, rs4796120 and rs3817655 variants was analyzed using SNPalyze software ver. 8.0 (Dynacom, Chiba, Japan).  $P < 0.05$  was considered significant.

## RESULTS

### Semiquantitative measurement of pretreatment serum cytokines in 31 randomly-selected patients

**A**T FIRST, TO identify cytokines/chemokines related to the treatment responses to PEG IFN/RBV therapy, semiquantitative measurement of the serum concentrations of 36 comprehensive cytokines/chemokines was performed by sandwich ELISA method by randomly selected patients. Next, to further confirm the result, cytokines showing the associations with the response were measured more precisely by bead array method in all patients.

In the first analysis, 31 patients were randomly selected from the 96 patients. The clinical characteristics of these 31 patients at the start of the therapy are shown in Table 1. Significant differences in the clinical backgrounds between those who did and those who did not



**Table 1** Baseline characteristics of the 31 patients analyzed using the sandwich ELISA method

Factor	SVR ( <i>n</i> = 20)	Non-SVR ( <i>n</i> = 11)	<i>P</i> -value
Age (years)	52 ± 11†	57 ± 10	0.25‡
Sex (male : female)	11:9	6:5	0.64§
Bodyweight (kg)	60.9 ± 9.6†	61.9 ± 13.9	0.81‡
Body mass index (kg/m <sup>2</sup> )	22.6 (18.9–31.3)¶	22.7 (17.5–26.8)	0.87††
History of IFN therapy (%)	30	36	0.78§
ALT (IU/L)	130 ± 100†	75 ± 35	0.09‡
AST (IU/L)	76 (22–331)¶	64 (24–178)	0.73††
γ-GTP (IU/L)	40 (12–289)	52 (24–137)	0.17††
Albumin (g/dL)	4.1 (3.7–4.5)	4.0 (3.0–4.7)	0.46††
Total cholesterol (mg/dL)	170 ± 24†	149 ± 33	0.06‡
HbA1c (%)	5.3 ± 0.5	5.3 ± 0.6	0.95‡
Creatinine (mg/dL)	0.71 ± 0.15	0.68 ± 0.15	0.54‡
WBC count (/μL)	4561 ± 1631	4056 ± 1277	0.38‡
Neutrophil count (/μL)	2130 (820–4200)¶	1500 (800–2700)	0.02††
Hemoglobin (g/dL)	14.5 ± 1.0†	13.8 ± 1.6	0.15‡
Platelet count (×10 <sup>3</sup> /μL)	16.4 ± 5.4	12.2 ± 3.9	0.03‡
α-Fetoprotein (ng/mL)	4.6 (1.4–28.9)¶	22.3 (11.4–79.7)	0.00005††
HCV RNA (KIU/mL)	1520 ± 1079†	2146 ± 899	0.11‡
Fibrosis (F1/F2/F3/F4)‡‡	14/1/1/2	3/2/2/3	0.02††
Activity (A1/A2/A3)‡‡	12/5/1	3/5/2	0.06††

†Mean ± standard deviation.

‡Student's *t*-test.

§Fisher's exact probability test.

¶Median (range).

††Mann-Whitney *U*-test.‡‡SVR, *n* = 18; non-SVR, *n* = 10.

Activity, the score of activity in liver biopsies; ALT, alanine aminotransferase; AST, aspartate aminotransferase; ELISA, enzyme-linked immunoassay; fibrosis, the score of fibrosis in liver biopsies; HbA1c, hemoglobin A1c; HCV, hepatitis C virus; SVR, sustained virological response; WBC, white blood cell; γ-GTP, γ-glutamyl transpeptidase.

achieve SVR were neutrophil counts, platelet counts, serum α-fetoprotein levels and the score of fibrosis in liver biopsies. Table 2 shows the difference in the cytokine/chemokine expression between the SVR and the non-SVR group. Because some cytokines/chemokines were below the measurement limit of the ELISA kit, as shown in Table 1, those cytokine/chemokines were not studied further. As shown here, the *RANTES* level was significantly higher in the SVR group than the non-SVR group (*P* = 0.048).

### Precise measurement of serum *RANTES* in all 96 patients

Because the semiquantitative measurement of pretreatment serum *RANTES* levels in 31 randomly selected patients demonstrated their significant correlation with the SVR, we determined the precise serum *RANTES* levels in all 96 patients using the bead array method and

investigated the correlation between those concentrations and the treatment outcome. The clinical characteristics of the 96 patients are shown in Table 3. Significant differences were seen between those with and without SVR in platelet count, viral loads and the liver fibrosis score, but there was no apparent difference in the total doses of PEG IFN and RBV. As shown in Figure 1, the distribution of serum *RANTES* levels in each treatment response differed significantly; the median serum *RANTES* level in the SVR group was significantly higher than that in the non-SVR group. Successive ROC analysis confirmed a significant association of the serum *RANTES* level with SVR, and the cut-off value of 3400 pg/mL to be most appropriate (Table 4). Using the cut-off value of 3400 pg/mL, 50.9% sensitivity, 79.5% specificity, 78.4% positive predictive value and 52.5% negative predictive value (area under the ROC, 0.643) were obtained for the prediction of SVR by serum *RANTES* level.

**Table 2** Difference in cytokine and chemokine expression between the SVR group and the non-SVR group in the 31 patients

Cytokine/chemokine	SVR (n = 20)	Non-SVR (n = 11)	P-value
RANTES	4.99 (0.25–8.32)†	1.24 (0.17–8.01)	0.048‡
MIF	1.31 (0.06–3.31)†	0.45 (0.08–2.67)	0.0630
IL-1ra	0.09 (0.00–3.30)†	0.07 (0.00–2.05)	0.2300
PAI-1	3.10 (0.35–7.34)†	2.73 (0.46–8.42)	0.3900
sICAM-1	3.18 (0.37–8.33)†	2.78 (0.74–10.3)	0.4800
IL-23	0.08 (0.01–0.78)†	0.07 (0.00–0.38)	0.5900
IL-27	0.05 (0.02–0.18)†	0.05 (0.00–0.23)	0.6500
IL-6	0.08 (0.01–3.22)†	0.10 (0.00–1.36)	0.7100
C5a	0.21 (0.01–2.72)†	0.12 (0.00–1.67)	0.7700
IFN- $\gamma$	0.07 (0.02–0.31)†	0.08 (0.00–0.40)	0.8000
CCL4	0.04 (0.01–3.08)†	0.05 (0.00–0.69)	0.8400
IL-32 $\alpha$	0.04 (0.00–0.71)†	0.07 (0.00–0.20)	0.9000
IL-8	0.16 (0.05–2.61)†	0.17 (0.03–2.21)	0.9300
IL-1 $\alpha$			N.A.
IL-1 $\beta$			N.A.
IL-2			N.A.
IL-4			N.A.
IL-5			N.A.
IL-10			N.A.
IL-12 p70			N.A.
IL-13			N.A.
IL-16			N.A.
IL-17			N.A.
IL-17E			N.A.
CCL1			N.A.
CCL2			N.A.
CCL3			N.A.
CXCL1			N.A.
CXCL11			N.A.
CXCL12			N.A.
CD154			N.A.
G-CSF			N.A.
GM-CSF			N.A.
IP-10			N.A.
TNF- $\alpha$			N.A.
sTREM-1			N.A.

†Median (range).

‡Mann–Whitney *U*-test.

N.A., not available; SVR, sustained virological response.

### Correlation between serum RANTES level and clinical parameters

Spearman's correlation coefficients between the pre-treatment serum RANTES level and clinical parameters in all 96 patients are shown in Table 5. As a result, a significant negative correlation with aspartate aminotransferase level and a significant positive correlation with platelet count were found, while no significant correlation was observed in other clinical parameters.

### Univariate and multivariate analysis of factors related to SVR

Univariate and multivariate analyses were performed successively in order to clarify the factors related to SVR. The viral factors included in the analysis were the ISDR and core a.a. 70 and 91, along with the host factor, IL-28B SNP. Those factors, conventional clinical background factors and serum RANTES levels were subjected to univariate and multivariate analysis. In the univariate